

# Understanding elemental anomalies in Globular Clusters: Experimental study of the $^{30}\text{Si}(p,\gamma)^{31}\text{P}$ reaction

Djamila Sarah HARROUZ

Supervisors:  
Nicolas de Séréville  
Faïrouz Hammache

# Globular Clusters

- Gravitationally bound systems of  $10^5$  to  $10^7$  stars, located in halo of spiral galaxies.
- Among the oldest structures in the Universe (age  $> 10$  Gyr).



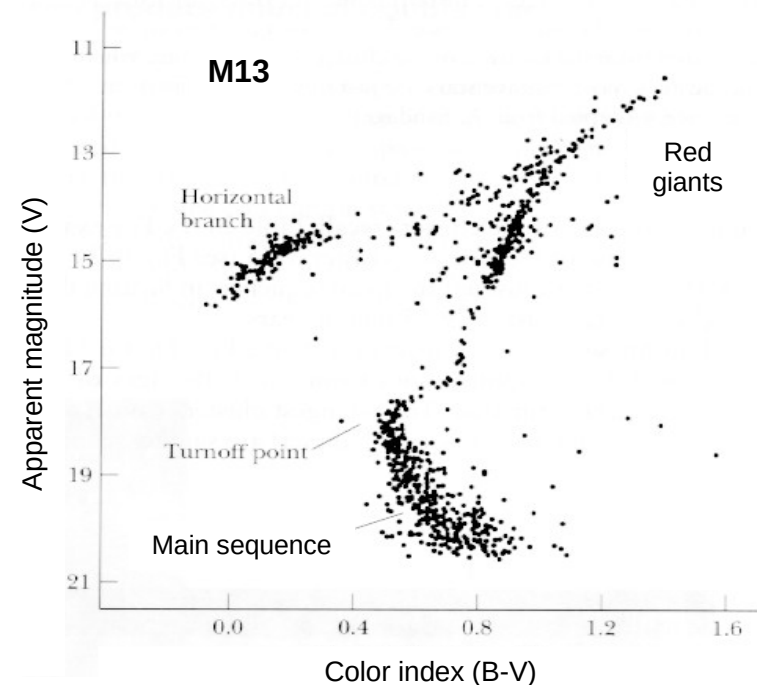
# Globular Clusters

- Gravitationally bound systems of  $10^5$  to  $10^7$  stars, located in halo of spiral galaxies.
- Among the oldest structures in the Universe (age > 10 Gyr).
- Globular Clusters are important for:
  - Cosmology (age of the Universe)
  - Galactic physics (formation and early evolution of galaxies)



# Globular Clusters

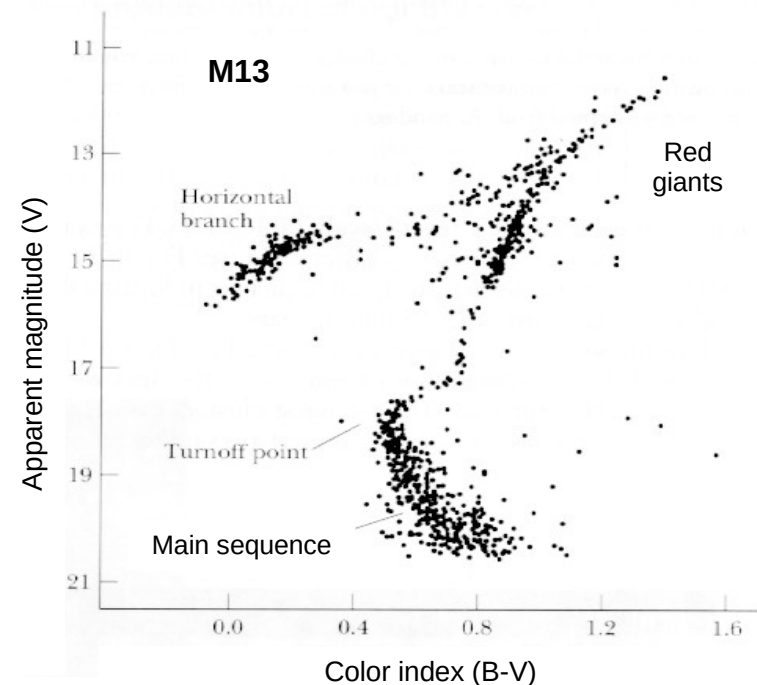
- Gravitationally bound systems of  $10^5$  to  $10^7$  stars, located in halo of spiral galaxies.
- Among the oldest structures in the Universe (age  $> 10$  Gyr).
- Globular Clusters are important for:
  - Cosmology (age of the Universe)
  - Galactic physics (formation and early evolution of galaxies)
- Low mass stars mainly on the **Main Sequence** and **Red Giant** branch.
  - Hydrogen-burning





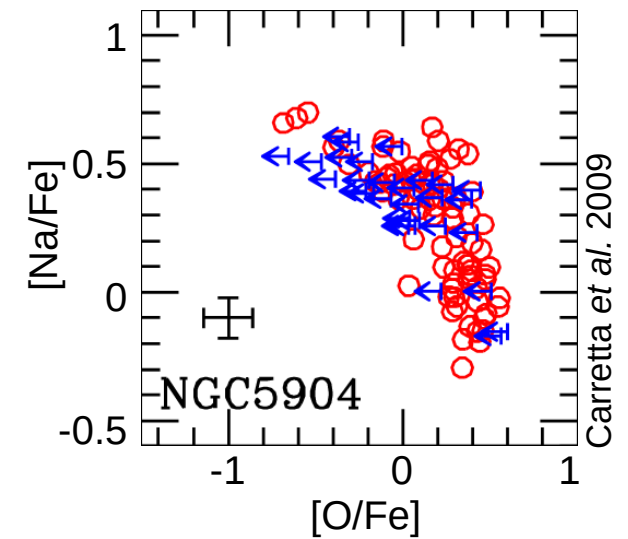
# Globular Clusters

- Gravitationally bound systems of  $10^5$  to  $10^7$  stars, located in halo of spiral galaxies.
- Among the oldest structures in the Universe (age > 10 Gyr).
- Globular Clusters are important for:
  - Cosmology (age of the Universe)
  - Galactic physics (formation and early evolution of galaxies)
- Low mass stars mainly on the **Main Sequence** and **Red Giant** branch.
  - Hydrogen-burning
- Paradigm: **Single stellar population**: same age and chemical composition.



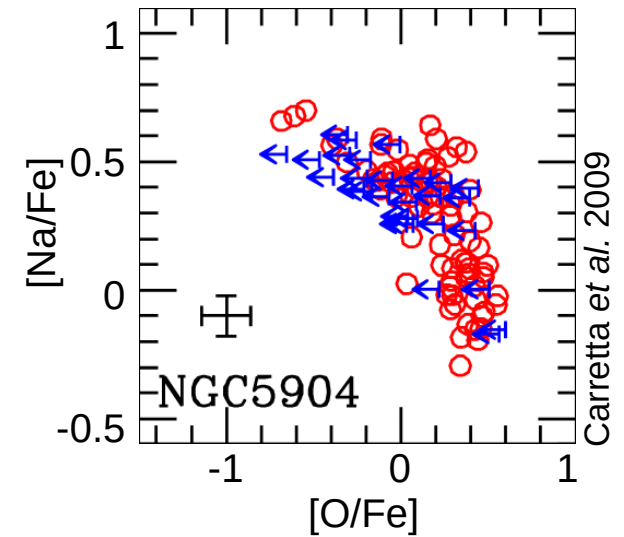
# Abundance anomalies in Globular Clusters

- Spectroscopic observations in Red Giant stars:
  - Abundance anticorrelation for C-N, O-Na, Mg-Al
  - Abundances vary from star-to-star



# Abundance anomalies in Globular Clusters

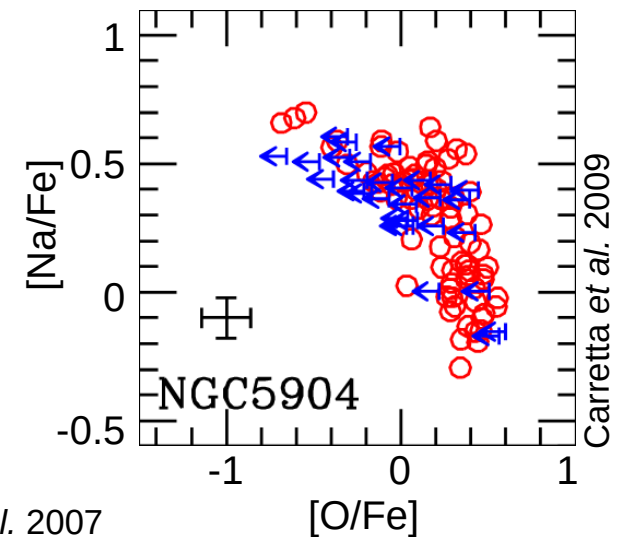
- Spectroscopic observations in Red Giant stars:
  - Abundance anticorrelation for C-N, O-Na, Mg-Al
  - Abundances vary from star-to-star
- Red giant stars temperature too low to alter abundances  
→ Abundances partially inherited from **unknown stars from previous generation, called polluters.**



# Abundance anomalies in Globular Clusters

- Spectroscopic observations in Red Giant stars:
  - Abundance anticorrelation for **C-N, O-Na, Mg-Al**
  - Abundances vary from star-to-star
- Red giant stars temperature too low to alter abundances  
→ Abundances partially inherited from **unknown stars from previous generation, called polluters.**

**Polluters must burn Hydrogen at  $T \sim 75$  MK** (Prantzos *et al.* 2007 & 2017)

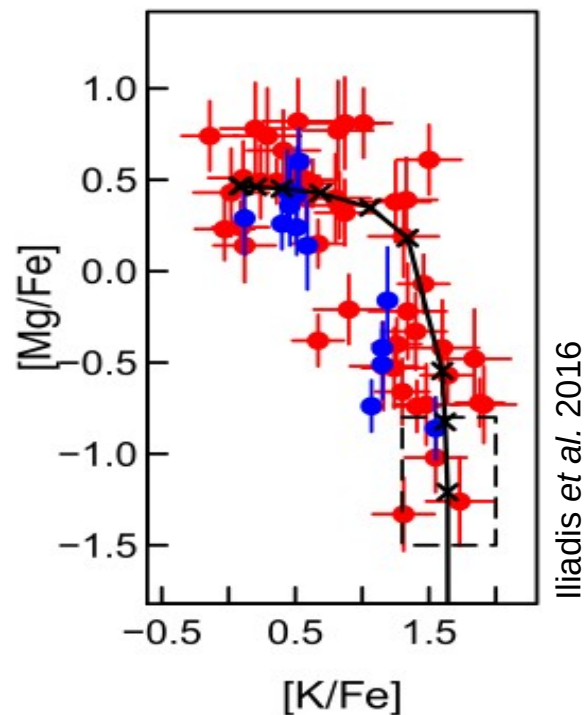
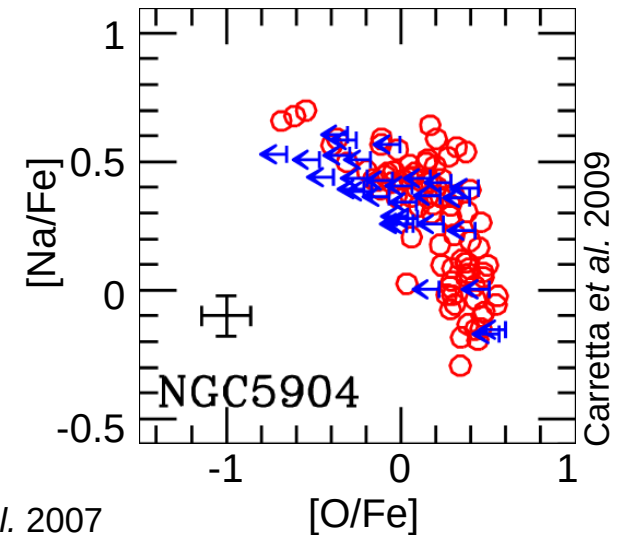




# Abundance anomalies in Globular Clusters

- Spectroscopic observations in Red Giant stars:
  - Abundance anticorrelation for **C-N**, **O-Na**, **Mg-Al**
  - Abundances vary from star-to-star
- Red giant stars temperature too low to alter abundances  
→ Abundances partially inherited from **unknown stars from previous generation, called polluters.**

**Polluters must burn Hydrogen at  $T \sim 75$  MK** (Prantzos *et al.* 2007 & 2017)



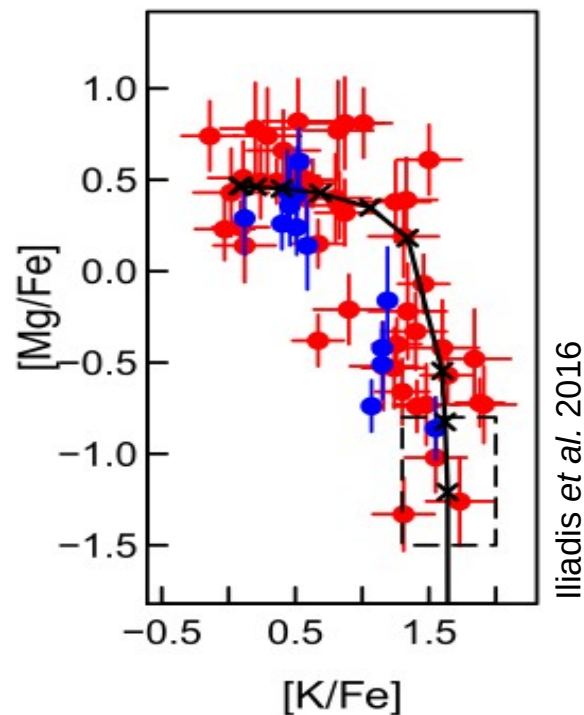
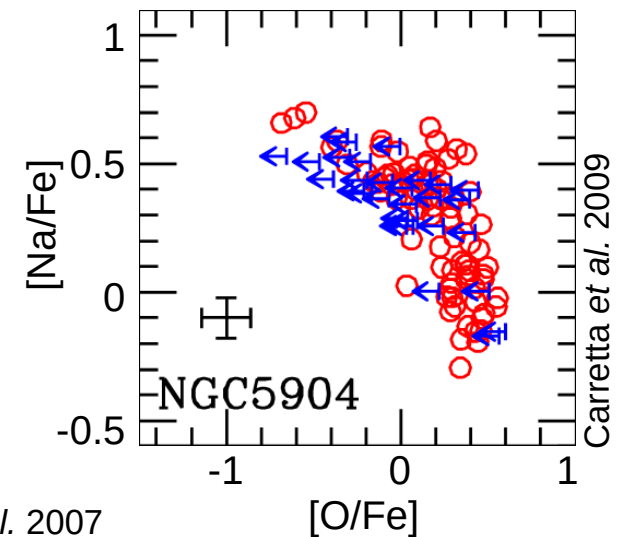
## Extreme case of NGC2419

- Observed **Mg-K** anticorrelation
- Requires much higher temperature in polluter site (between 100 MK and 200 MK) to overcome Coulomb barrier in proton capture reactions.

# Abundance anomalies in Globular Clusters

- Spectroscopic observations in Red Giant stars:
  - Abundance anticorrelation for **C-N**, **O-Na**, **Mg-Al**
  - Abundances vary from star-to-star
- Red giant stars temperature too low to alter abundances  
→ Abundances partially inherited from **unknown stars from previous generation, called polluters.**

**Polluters must burn Hydrogen at  $T \sim 75$  MK** (Prantzos *et al.* 2007 & 2017)

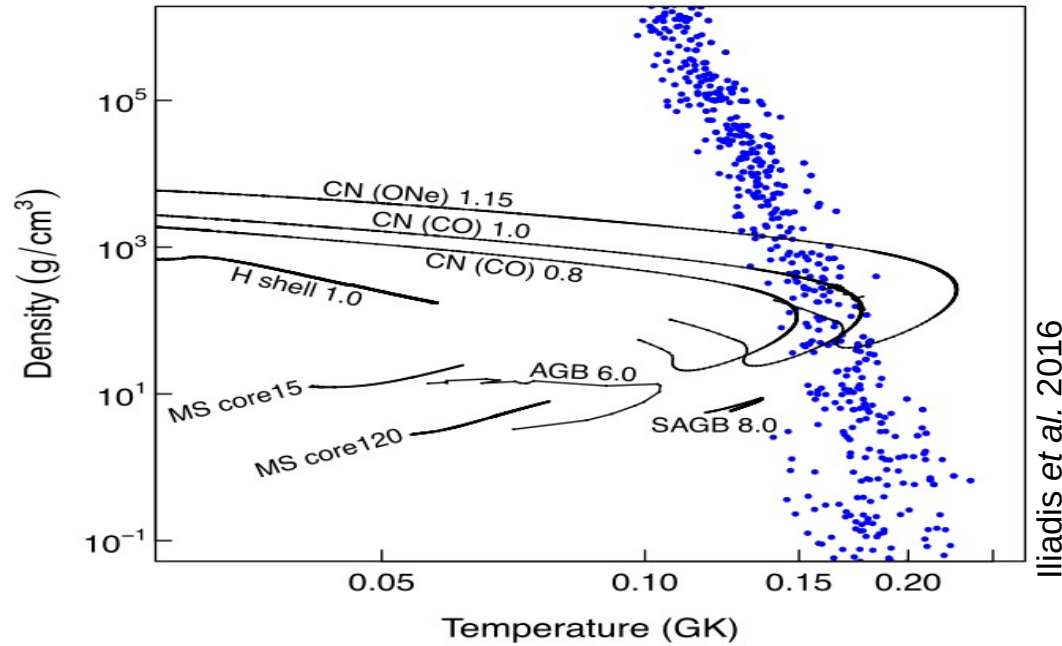


## Extreme case of NGC2419

- Observed **Mg-K** anticorrelation
- Requires much higher temperature in polluter site (between 100 MK and 200 MK) to overcome Coulomb barrier in proton capture reactions.

**What is the nature and type of polluter stars? ( $T, \rho$ )?**

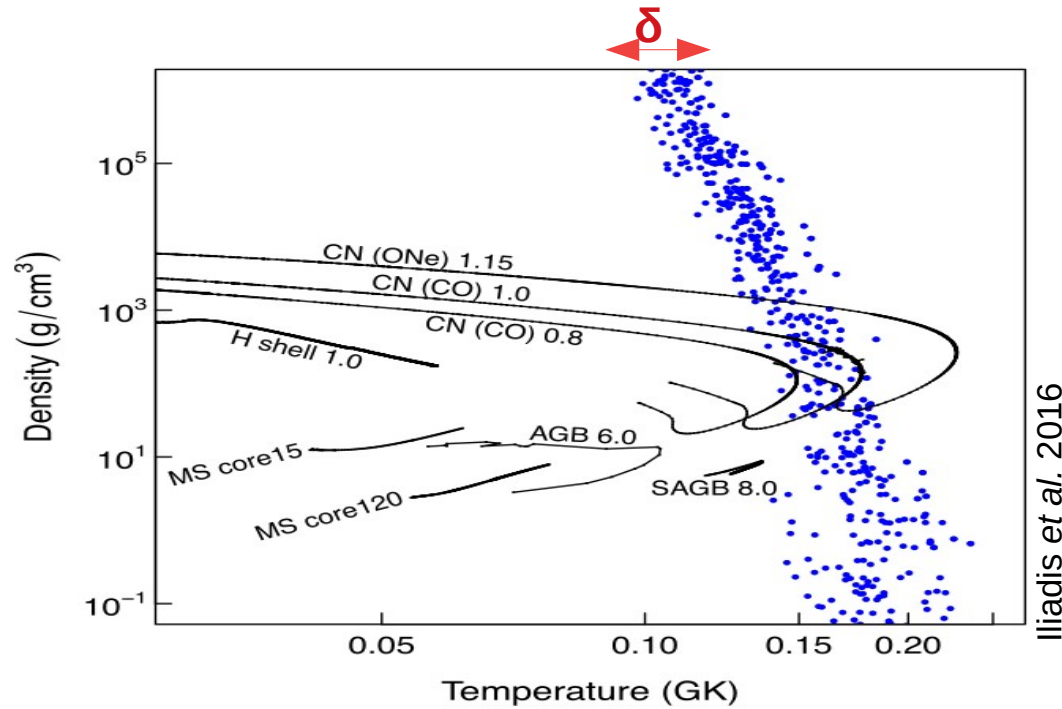
# NGC2419 Abundances



## Sensitivity Studies

- Simulate nucleosynthesis reaction network in **H-burning conditions** (with Monte Carlo calculation) for uniform **T** and  **$\rho$**  distributions, and varying reaction rates within uncertainties.

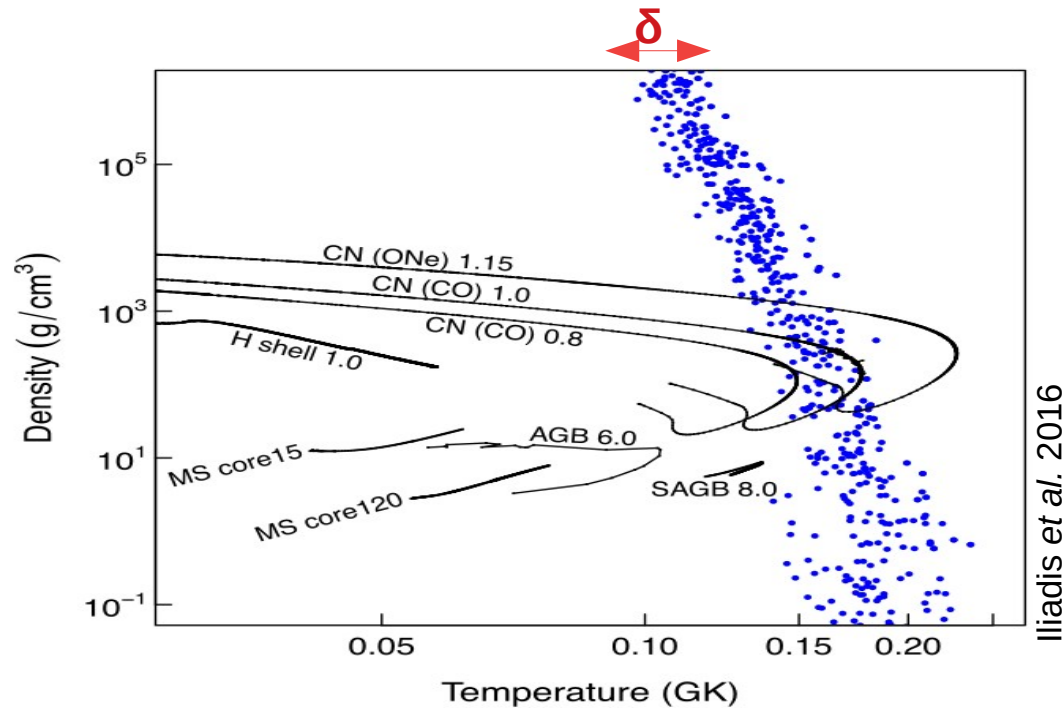
# NGC2419 Abundances



## Sensitivity Studies

- Simulate nucleosynthesis reaction network in **H-burning conditions** (with Monte Carlo calculation) for uniform **T** and  **$\rho$**  distributions, and varying reaction rates within uncertainties.
- Uncertainty on reaction rates  $\rightarrow$  T spread increased by 70%.

# NGC2419 Abundances

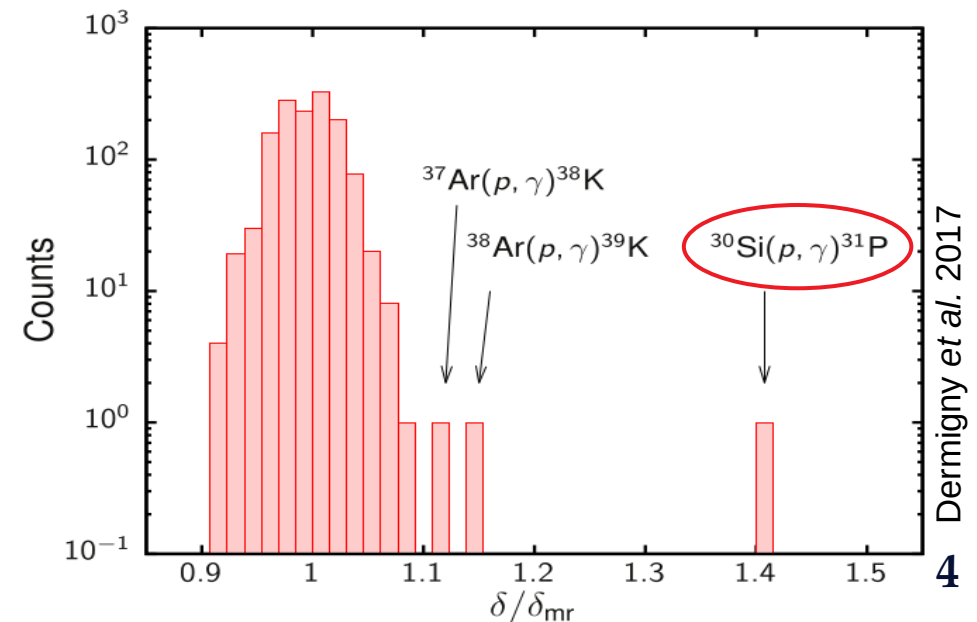


## Key Reactions

- Individual variation of reaction rates within their uncertainties.
- Impact of a few (p,γ) reactions.
- $^{30}\text{Si}(p,\gamma)^{31}\text{P}$  reaction contributes the most to the spread of the (T, ρ) locus for  $100 \text{ MK} < T < 200 \text{ MK}$

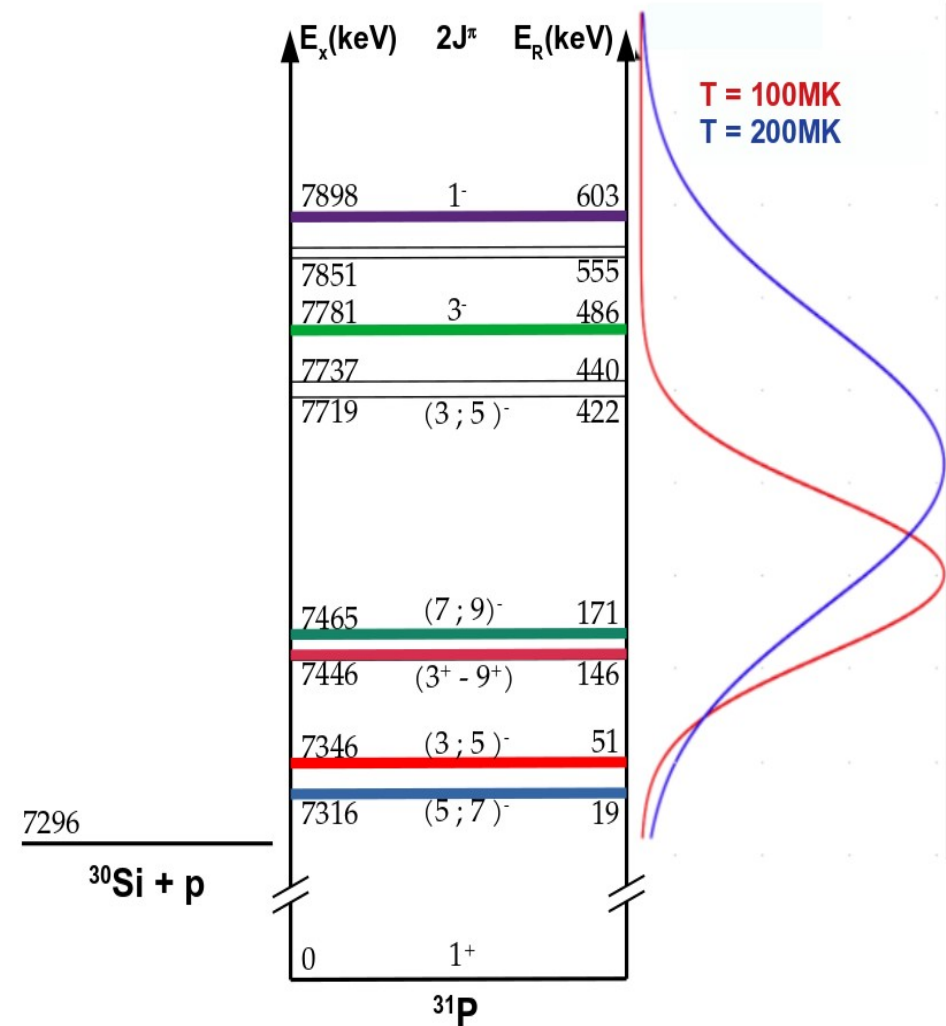
## Sensitivity Studies

- Simulate nucleosynthesis reaction network in **H-burning conditions** (with Monte Carlo calculation) for uniform **T** and **ρ** distributions, and varying reaction rates within uncertainties.
- Uncertainty on reaction rates → T spread increased by 70%.



# State of the art for $^{30}\text{Si}(p,\gamma)^{31}\text{P}$ reaction

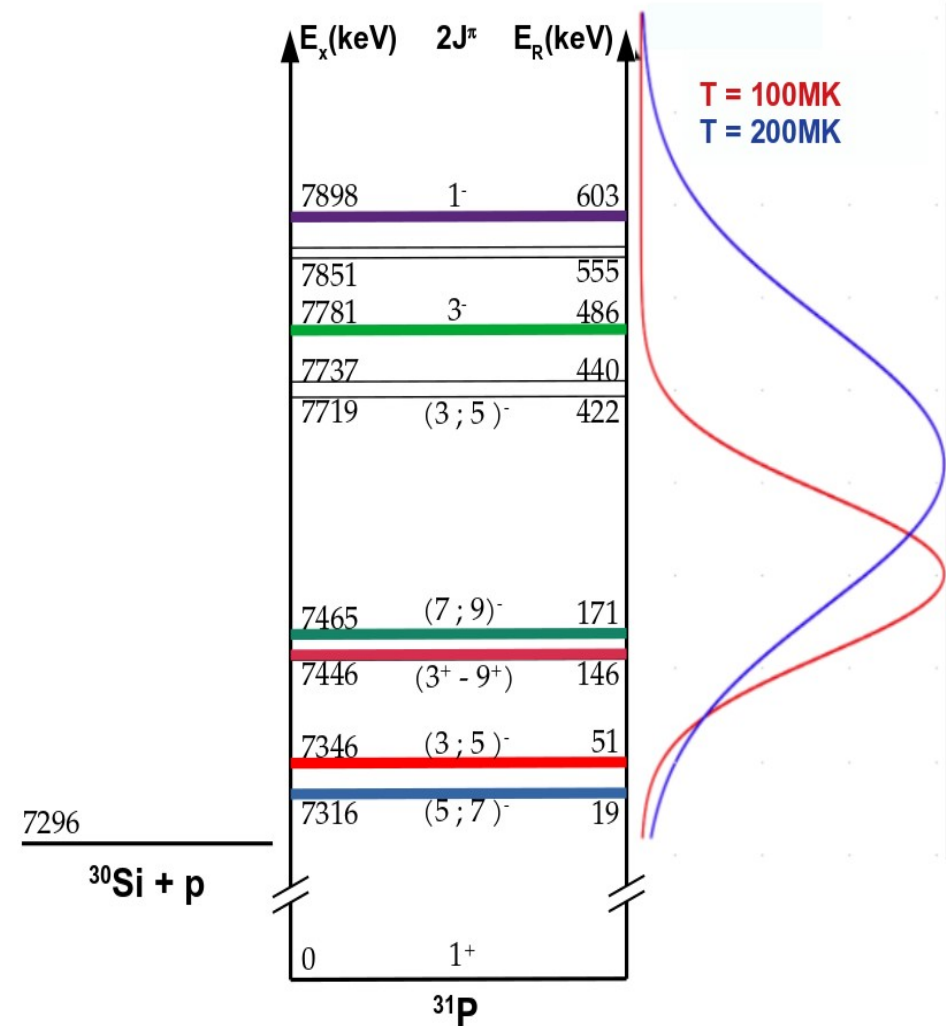
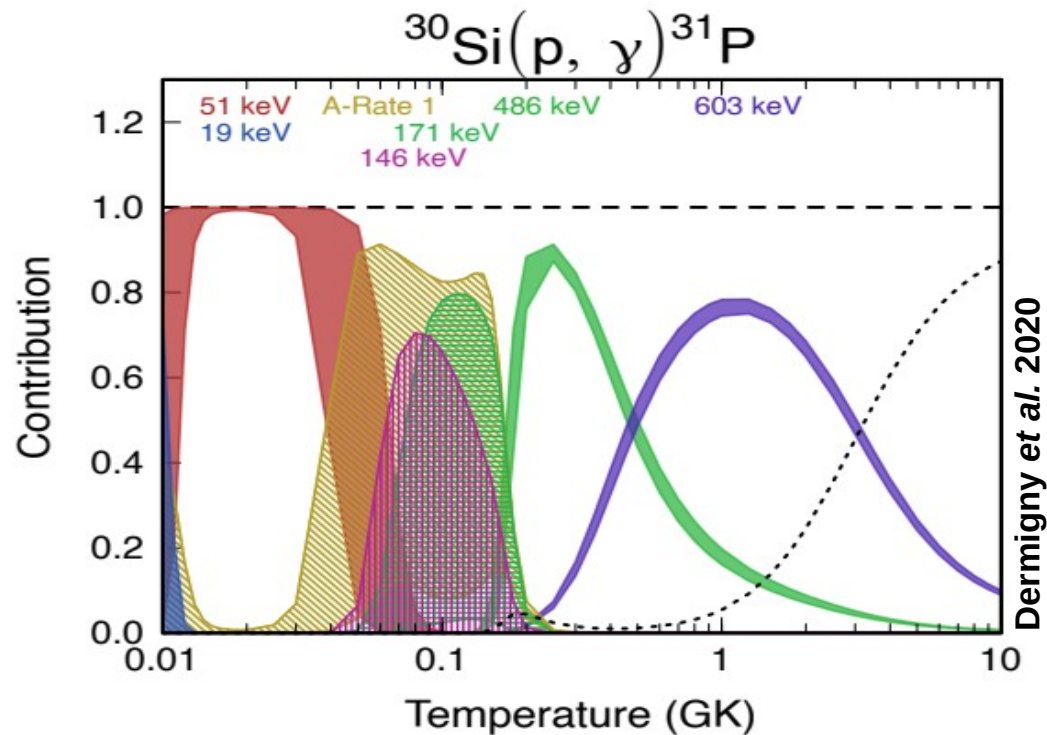
- Energies known with uncertainty better than 4 keV
- Spins and parities constrained but mostly unknown





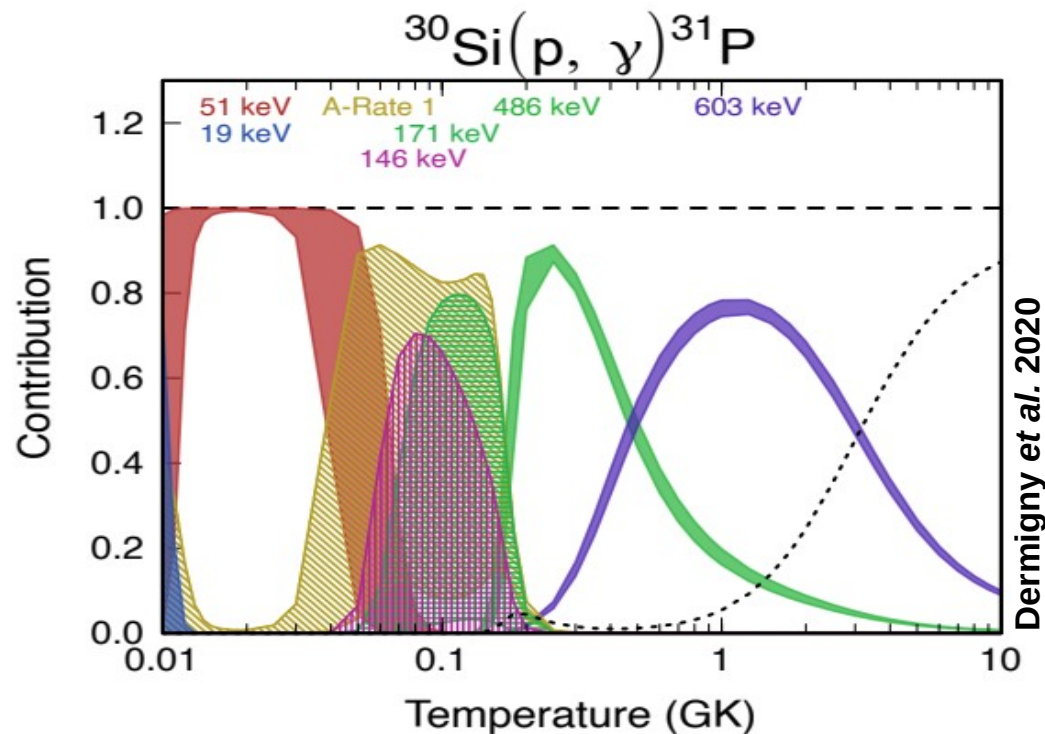
# State of the art for $^{30}\text{Si}(p,\gamma)^{31}\text{P}$ reaction

- Energies known with uncertainty better than 4 keV
- Spins and parities constrained but mostly unknown

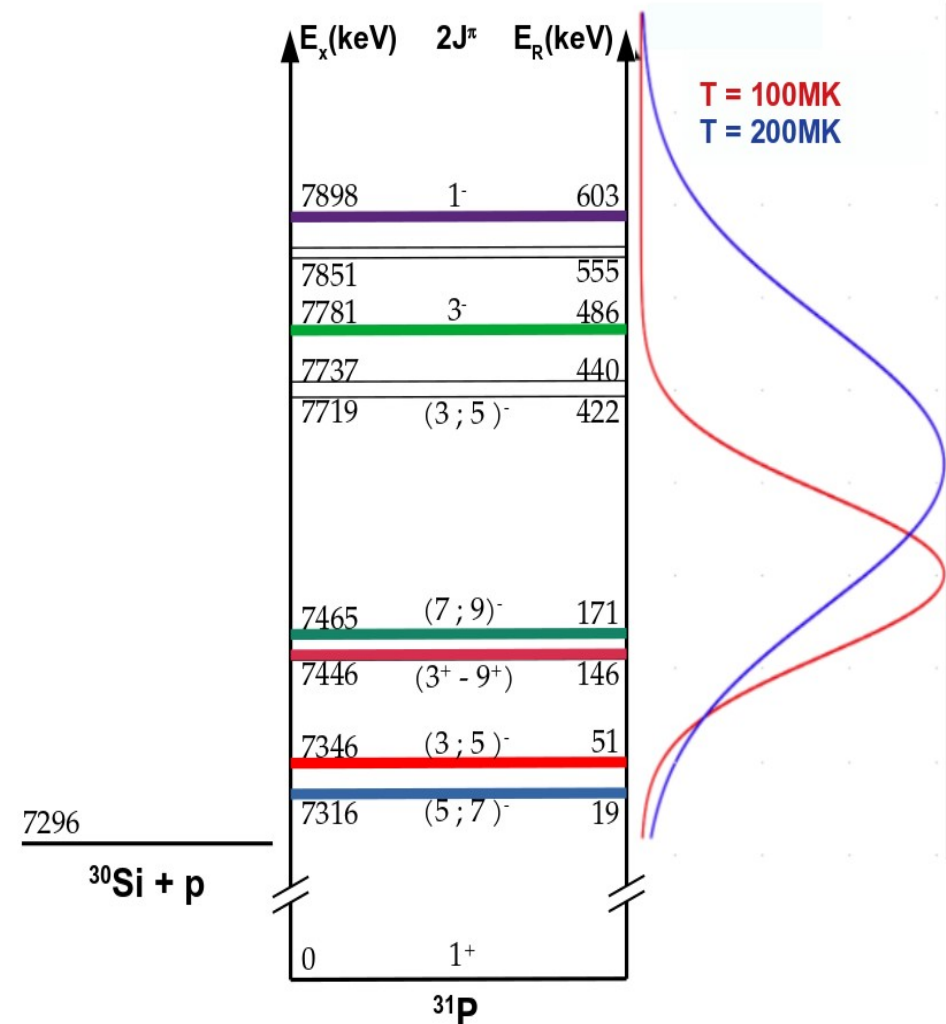


# State of the art for $^{30}\text{Si}(p,\gamma)^{31}\text{P}$ reaction

- Energies known with uncertainty better than 4 keV
- Spins and parities constrained but mostly unknown



- $E_r = 19$  keV:  $C^2S = 0.002$  (Vernotte et al. 1990)
- $E_r = 51$  and  $146$  keV: Mean reduced widths, systematic study  $\langle \theta^2 \rangle = 0.0003$
- $E_r = 171$  keV: Upper limit  $C^2S < 0.003$  (Dermigny et al. 2020)



- $E_r = 422, 486$  keV sole direct measurements using  $\gamma\gamma$  coincidences (Dermigny et al. 2020)
- $E_r = 603$  keV: several direct measurements, reference resonance

# Experimental Strategy

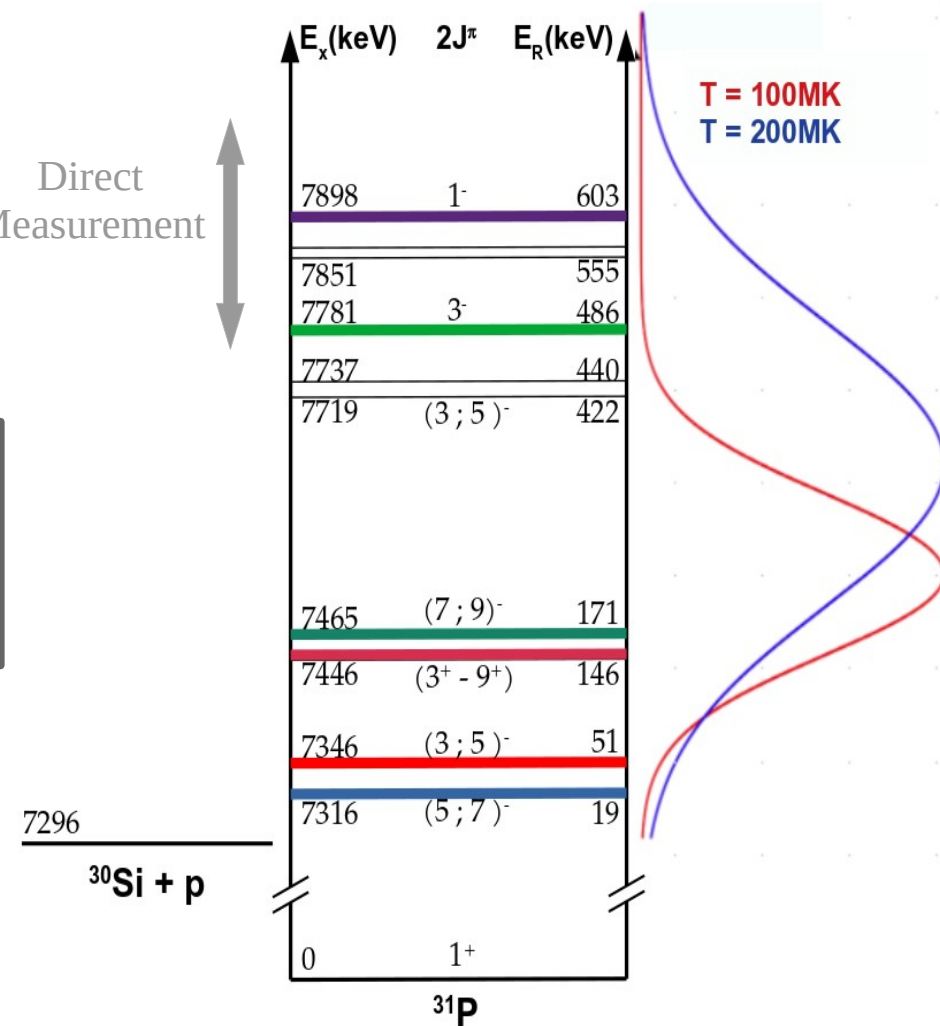
Thermonuclear reaction rate for single and isolated narrow resonance :

$$\langle \sigma v \rangle \propto (\omega \gamma) e^{(-E_R/kT)}$$

## High energy

- Direct measurement of resonance strength  $\omega \gamma$  @**DRAGON** (Triumf)
- Independent strength determination of high energy resonances.

Direct  
Measurement



# Experimental Strategy

Thermonuclear reaction rate for single and isolated narrow resonance :

$$\langle \sigma v \rangle \propto (\omega \gamma) e^{(-E_R/kT)}$$

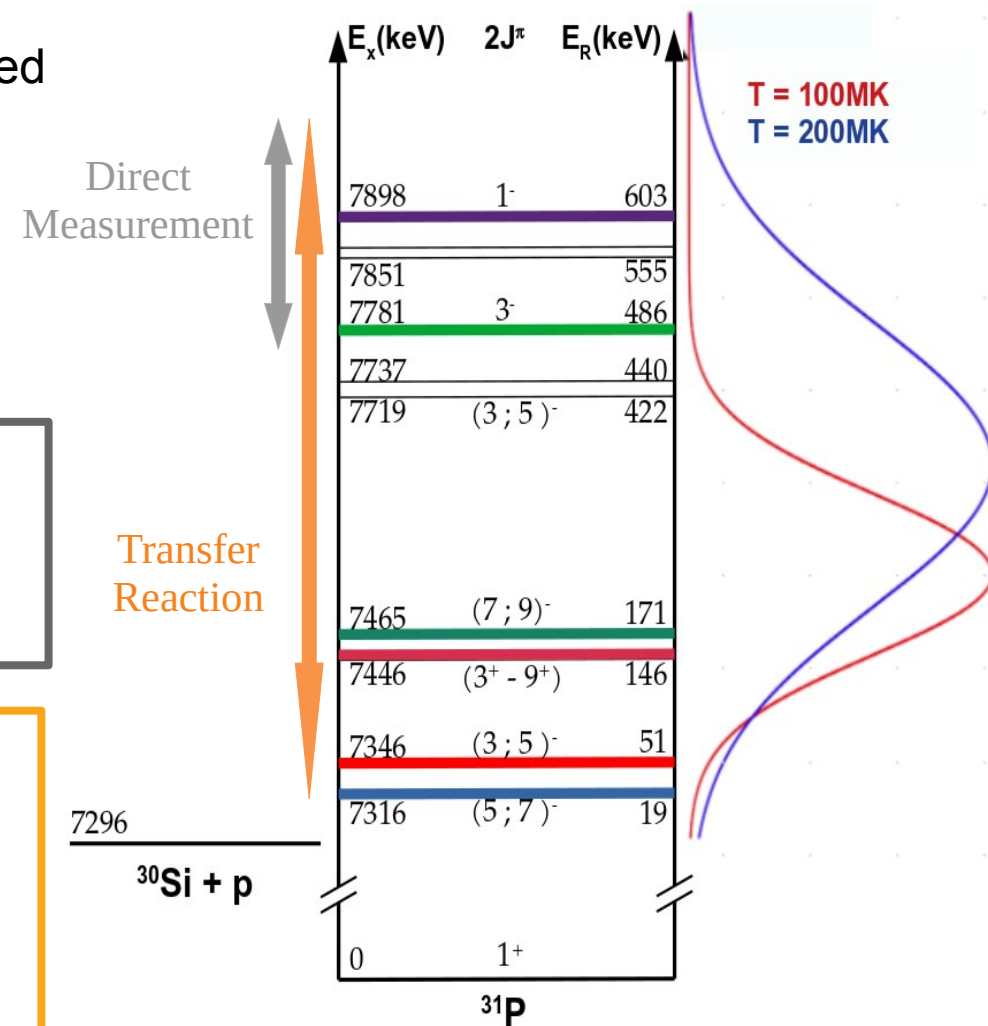
$$\omega \gamma = \frac{2J_R + 1}{(2J_p + 1)(2J_{30Si} + 1)} \frac{\Gamma_p \Gamma_\gamma}{\Gamma}$$

## High energy

- Direct measurement of resonance strength  $\omega \gamma$  @**DRAGON** (Triumf)
- Independent strength determination of high energy resonances.

## Low energy

$$\begin{cases} \Gamma = \Gamma_p + \Gamma_\gamma \\ \Gamma_p \ll \Gamma_\gamma \end{cases} \Rightarrow \omega \gamma \simeq \omega \Gamma_p$$



# Experimental Strategy

Thermonuclear reaction rate for single and isolated narrow resonance :

$$\langle \sigma v \rangle \propto (\omega \gamma) e^{(-E_R/kT)}$$

$$\omega \gamma = \frac{2J_R + 1}{(2J_p + 1)(2J_{30Si} + 1)} \frac{\Gamma_p \Gamma_\gamma}{\Gamma}$$

## High energy

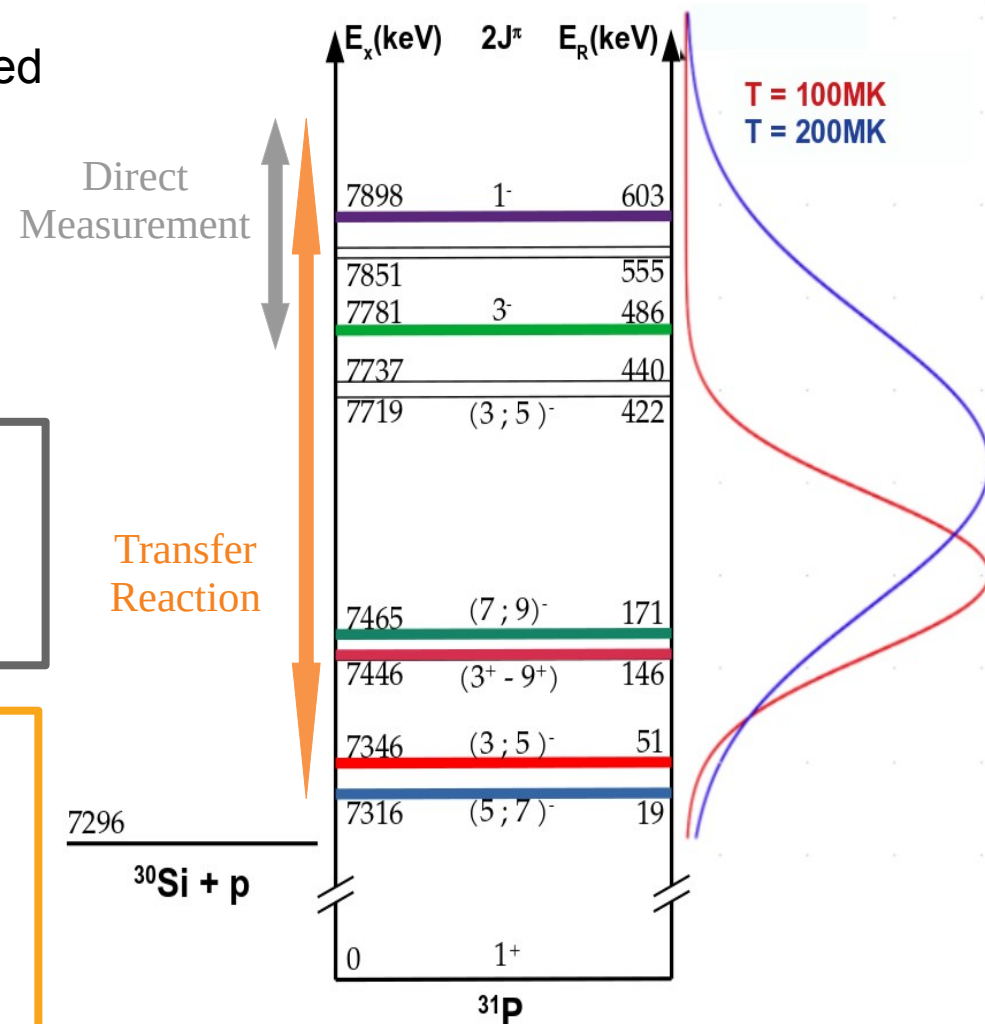
- Direct measurement of **resonance strength**  $\omega \gamma$  @**DRAGON** (Triumf)
- Independent strength determination of high energy resonances.

## Low energy

$$\begin{cases} \Gamma = \Gamma_p + \Gamma_\gamma \\ \Gamma_p \ll \Gamma_\gamma \end{cases} \Rightarrow \omega \gamma \simeq \omega \Gamma_p$$

## $^{30}\text{Si}(^3\text{He}, d)^{31}\text{P}$ transfer reaction

- Experiment by Vernotte in 1990 at Orsay's SplitPole: low statistics, limited resolution and contaminations.
- → new measurements @**Q3D** (MLL) with improved energy resolution and sensitivity.





# Transfer Reaction

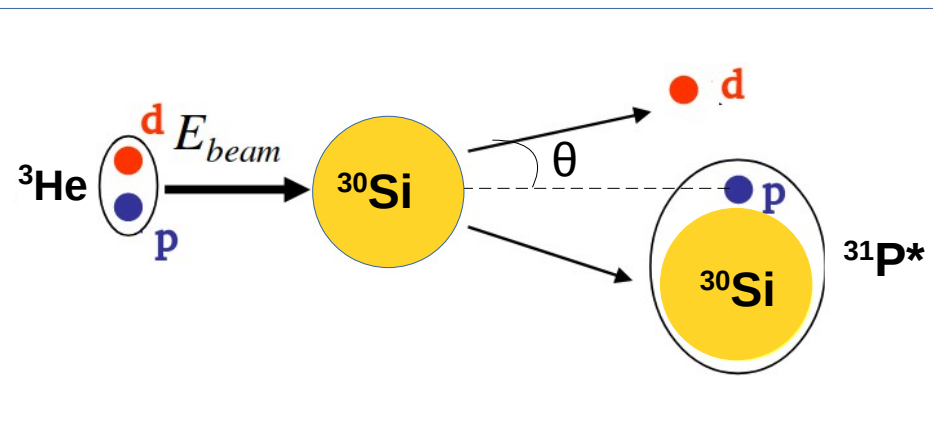




# One proton Transfer Reaction

(p, $\gamma$ ) can be studied through one proton ( $^3\text{He},d$ ) transfer reaction

Experimental method

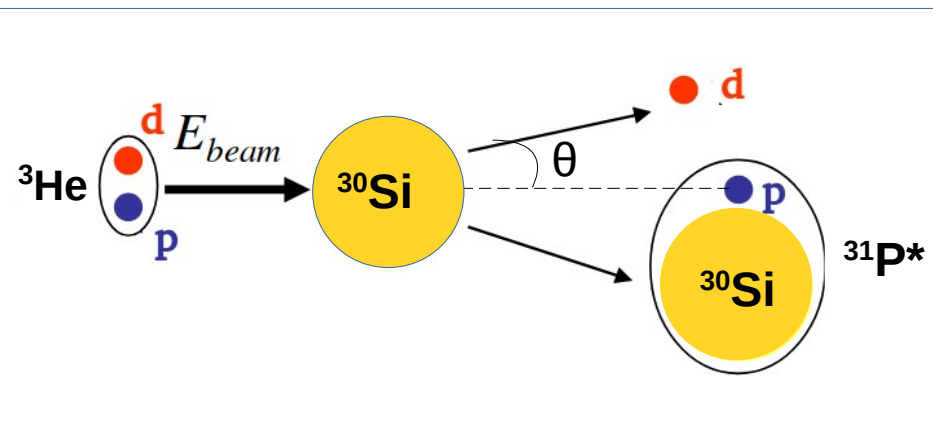


- Excitation energies
- Angular distribution

# One proton Transfer Reaction

$(p,\gamma)$  can be studied through one proton ( $^3\text{He},d$ ) transfer reaction

Experimental method



- Excitation energies
- Angular distribution

Theoretical model for direct transfer

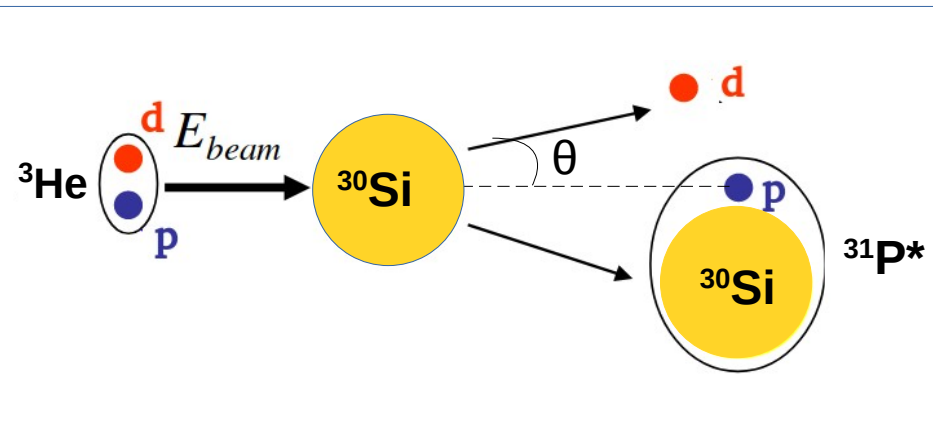
**Distorted Wave Born Approximation:**

- Elastic scattering dominates entrance and exit channels (described by optical models)
- Transfer 1<sup>st</sup> order perturbation
- No configuration rearrangement

# One proton Transfer Reaction

(p,γ) can be studied through one proton ( $^3\text{He},d$ ) transfer reaction

Experimental method



Theoretical model for direct transfer

**Distorted Wave Born Approximation:**

- Elastic scattering dominates entrance and exit channels (described by optical models)
- Transfer 1<sup>st</sup> order perturbation
- No configuration rearrangement

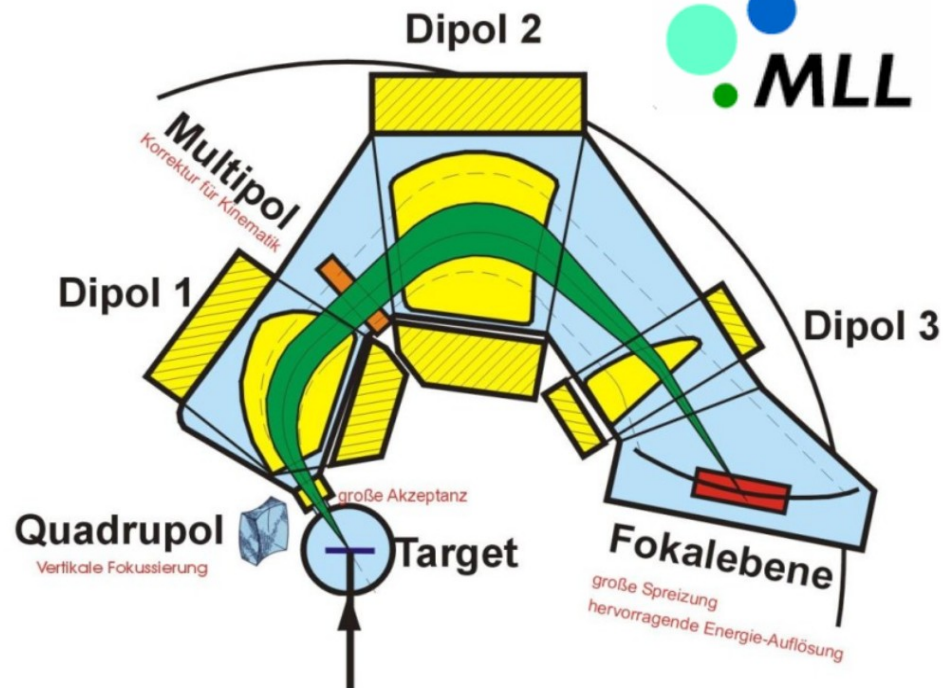
- Excitation energies
- Angular distribution

$$\frac{d\sigma}{d\Omega}(\theta)_{exp} = C^2 S \frac{d\sigma}{d\Omega}(\theta)_{DWBA}$$

$$\Gamma_p = C^2 S \Gamma_p^{s.p.}(E_r, \ell)$$

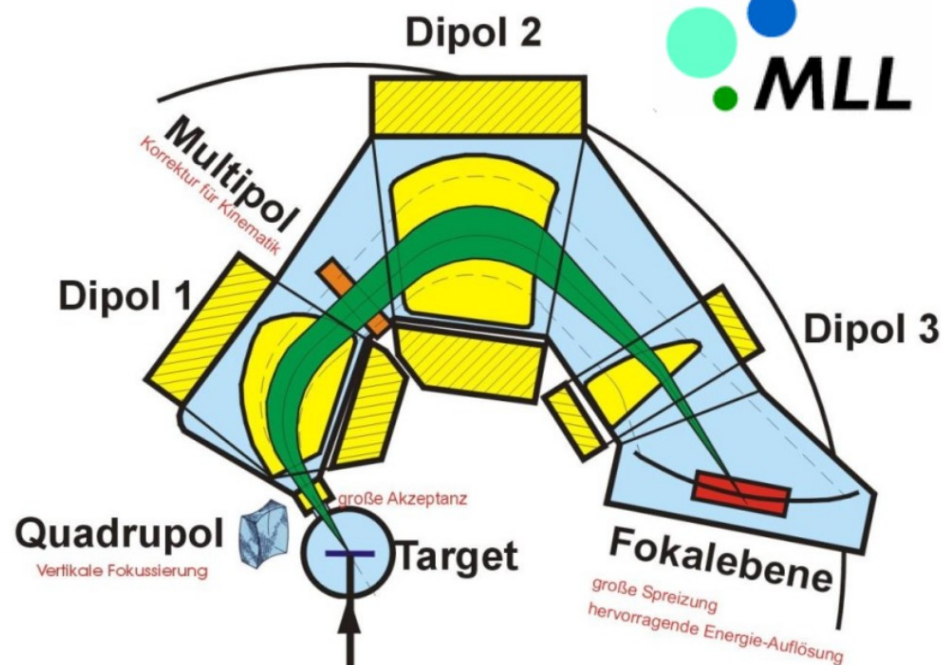
➡ Shape of the distribution  
→ transferred angular orbital momentum  $\ell$

# $^{30}\text{Si}(^3\text{He},d)^{31}\text{P}$ reaction @Q3D



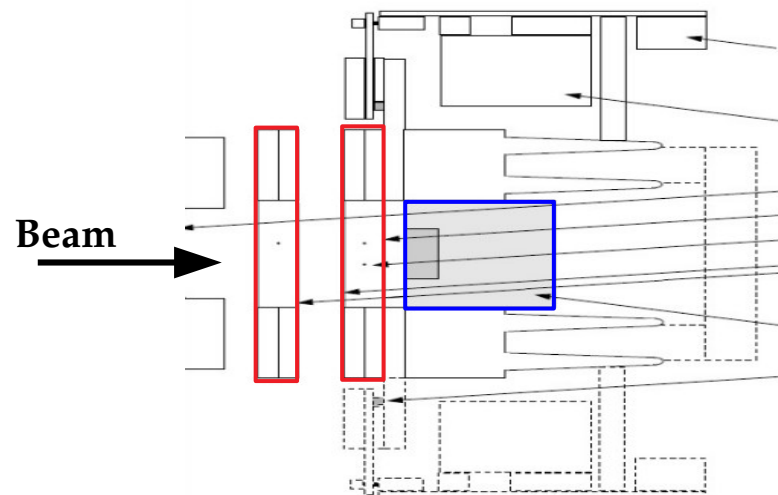
- Beam  $^3\text{He}$  :  $E = 25 \text{ MeV}$   
 $I = 200 \text{ nAe}$
- Targets:  $^{30}\text{SiO}_2$  ( $40 \mu\text{g}/\text{cm}^2$ ) enriched at 95% on  $^{\text{nat}}\text{C}$   
 $^{\text{nat}}\text{SiO}_2$  ( $20 \mu\text{g}/\text{cm}^2$ ) on  $^{\text{nat}}\text{C}$
- Solid Angle : 4 to 12 msr
- Energy resolution  $\frac{\Delta E}{E} \sim 2 \cdot 10^{-4}$

# $^{30}\text{Si}(^3\text{He},d)^{31}\text{P}$ reaction @Q3D



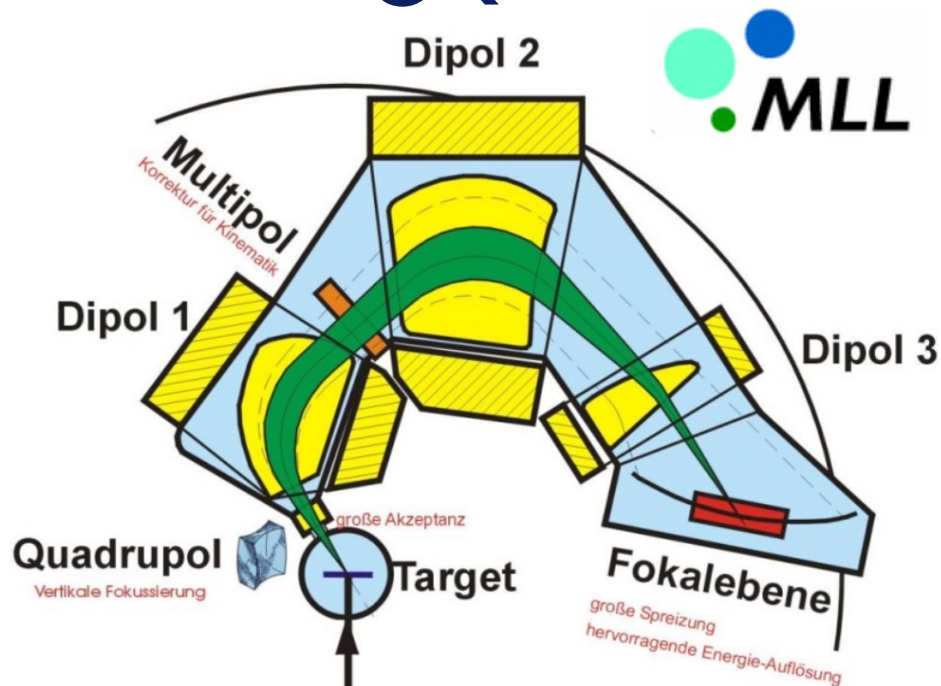
- Beam  $^3\text{He}$  :  $E = 25 \text{ MeV}$   
 $I = 200 \text{ nAe}$
- Targets:  $^{30}\text{SiO}_2$  ( $40 \mu\text{g}/\text{cm}^2$ ) enriched at 95% on  $^{\text{nat}}\text{C}$   
 $^{\text{nat}}\text{SiO}_2$  ( $20 \mu\text{g}/\text{cm}^2$ ) on  $^{\text{nat}}\text{C}$
- Solid Angle : 4 to 12 msr
- Energy resolution  $\frac{\Delta E}{E} \sim 2 \cdot 10^{-4}$

## Focal plane detectors :



- Single-wire proportional counters → position on the focal plane and energy loss.
- Plastic scintillator → residual energy.

# $^{30}\text{Si}(^3\text{He},d)^{31}\text{P}$ reaction @Q3D



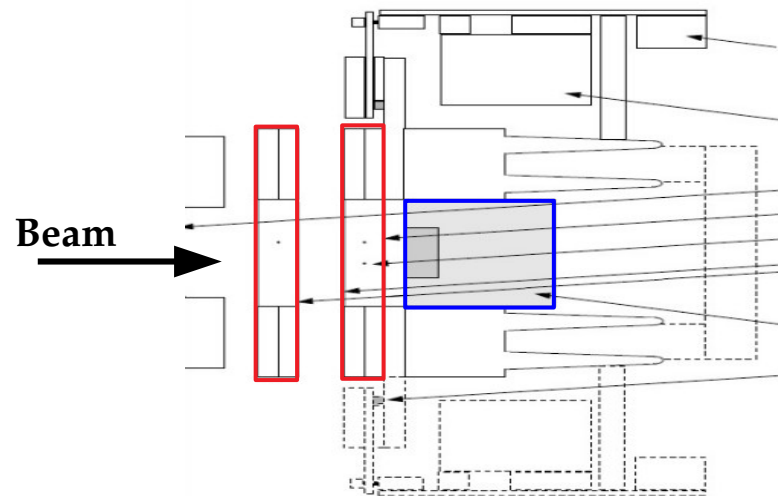
➤ Beam  $^3\text{He}$  :  $E = 25 \text{ MeV}$   
 $I = 200 \text{ nAe}$

➤ Targets:  $^{30}\text{SiO}_2$  ( $40 \mu\text{g}/\text{cm}^2$ ) enriched at 95% on  $^{\text{nat}}\text{C}$   
 $^{\text{nat}}\text{SiO}_2$  ( $20 \mu\text{g}/\text{cm}^2$ ) on  $^{\text{nat}}\text{C}$

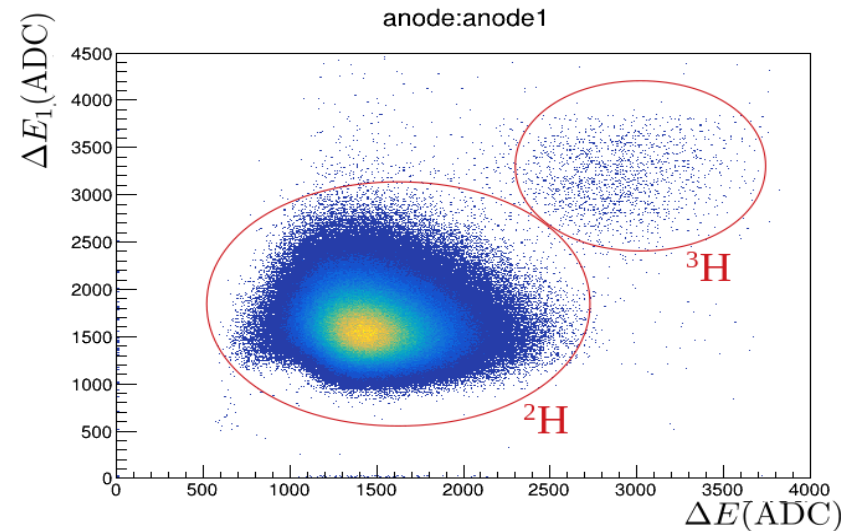
➤ Solid Angle : 4 to 12 msr

➤ Energy resolution  $\frac{\Delta E}{E} \sim 2 \cdot 10^{-4}$

## Focal plane detectors :

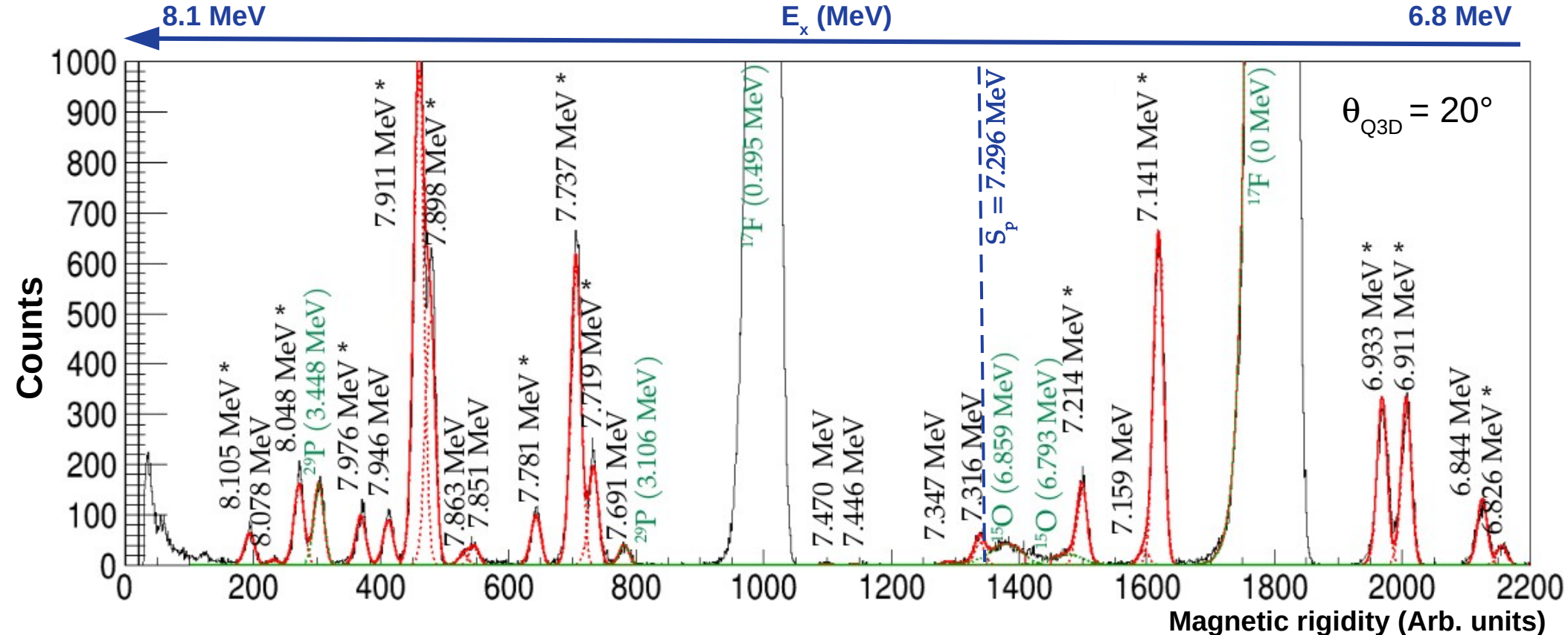


- Single-wire proportional counters → position on the focal plane and energy loss.
- Plastic scintillator → residual energy.



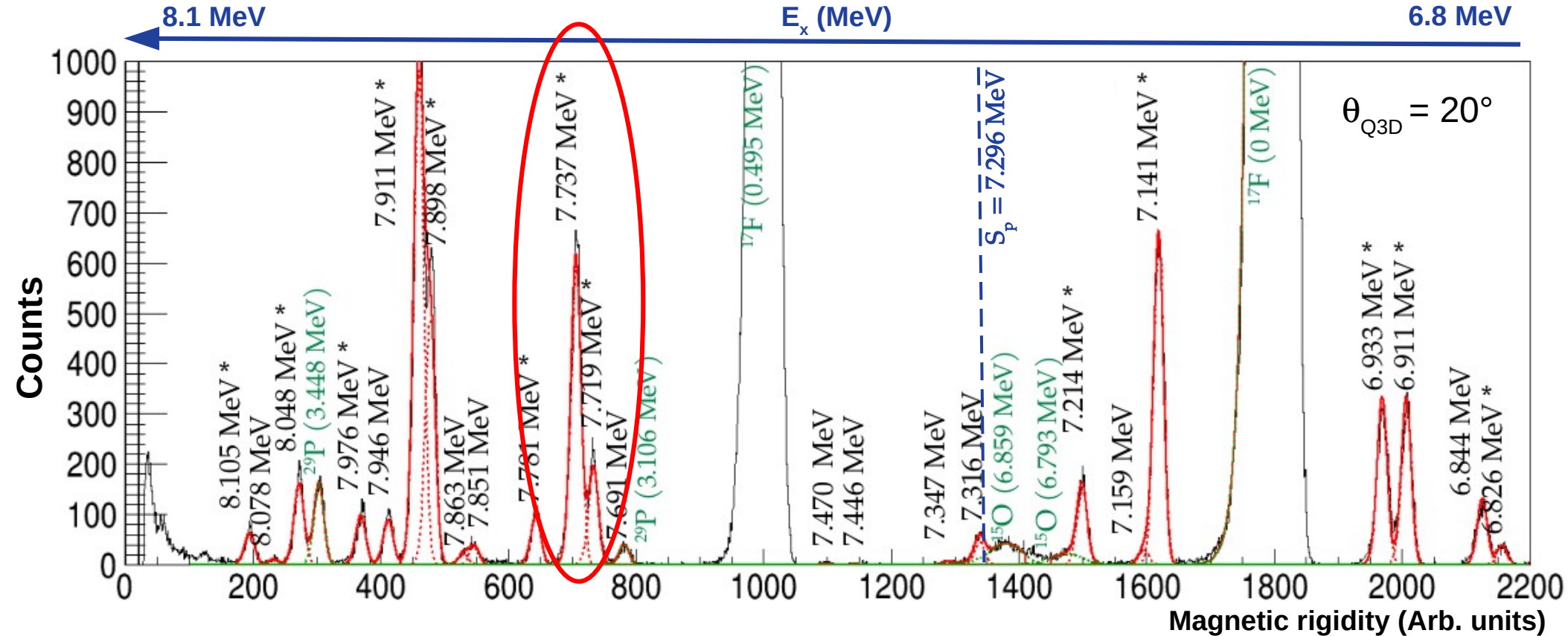


# Magnetic rigidity spectrum



- Spectra for 7 lab angles : 6°, 10°, 12°, 16°, 20°, 23°, 32°
- Fit with multiple skewed gaussians with common width.
- Experimental resolution **FWHM ~ 7 keV**  
Vernotte (1990) ~25 keV

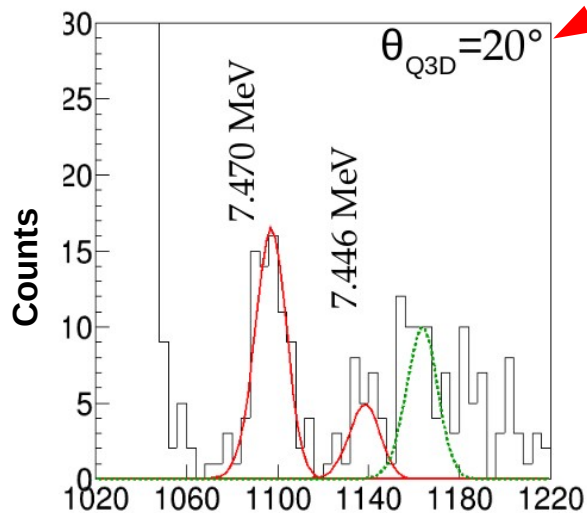
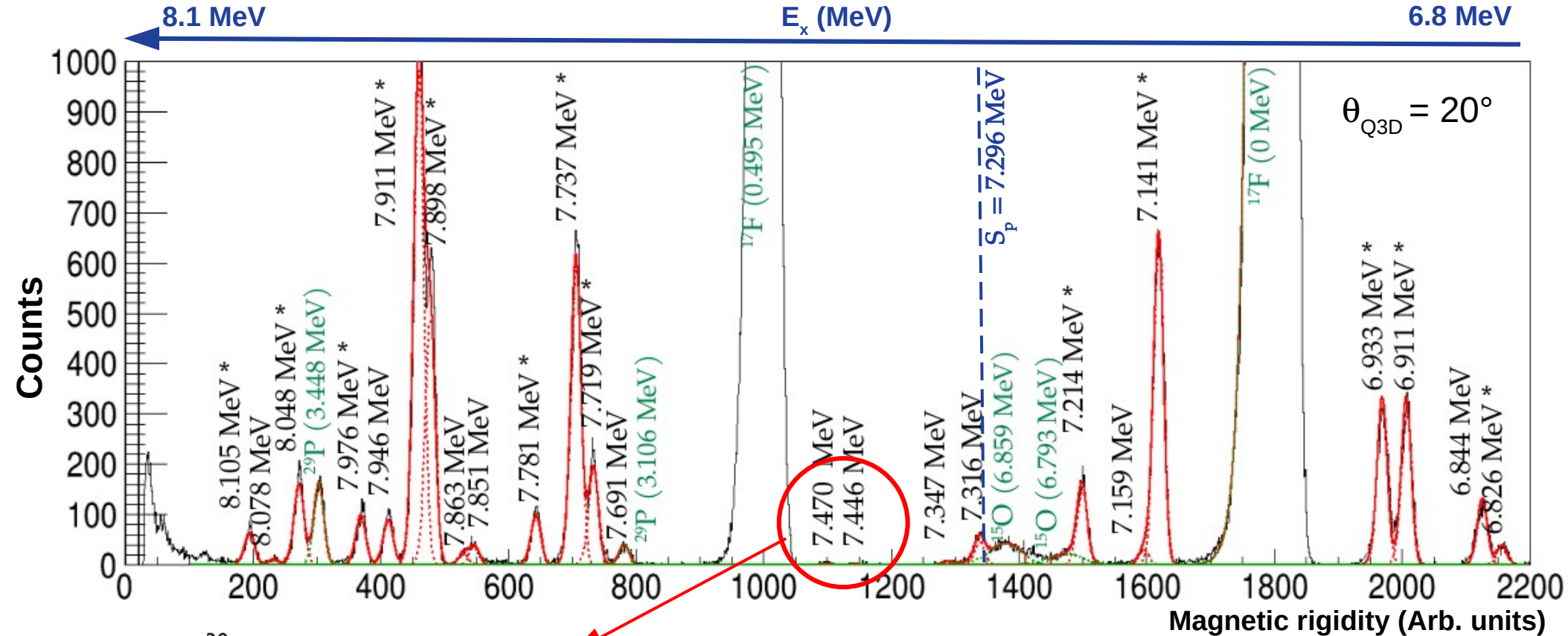
# Magnetic rigidity spectrum



- Spectra for 7 lab angles : 6°, 10°, 12°, 16°, 20°, 23°, 32°
- Fit with multiple skewed gaussians with common width.
- Experimental resolution **FWHM ~ 7 keV**  
Vernotte (1990) ~25 keV

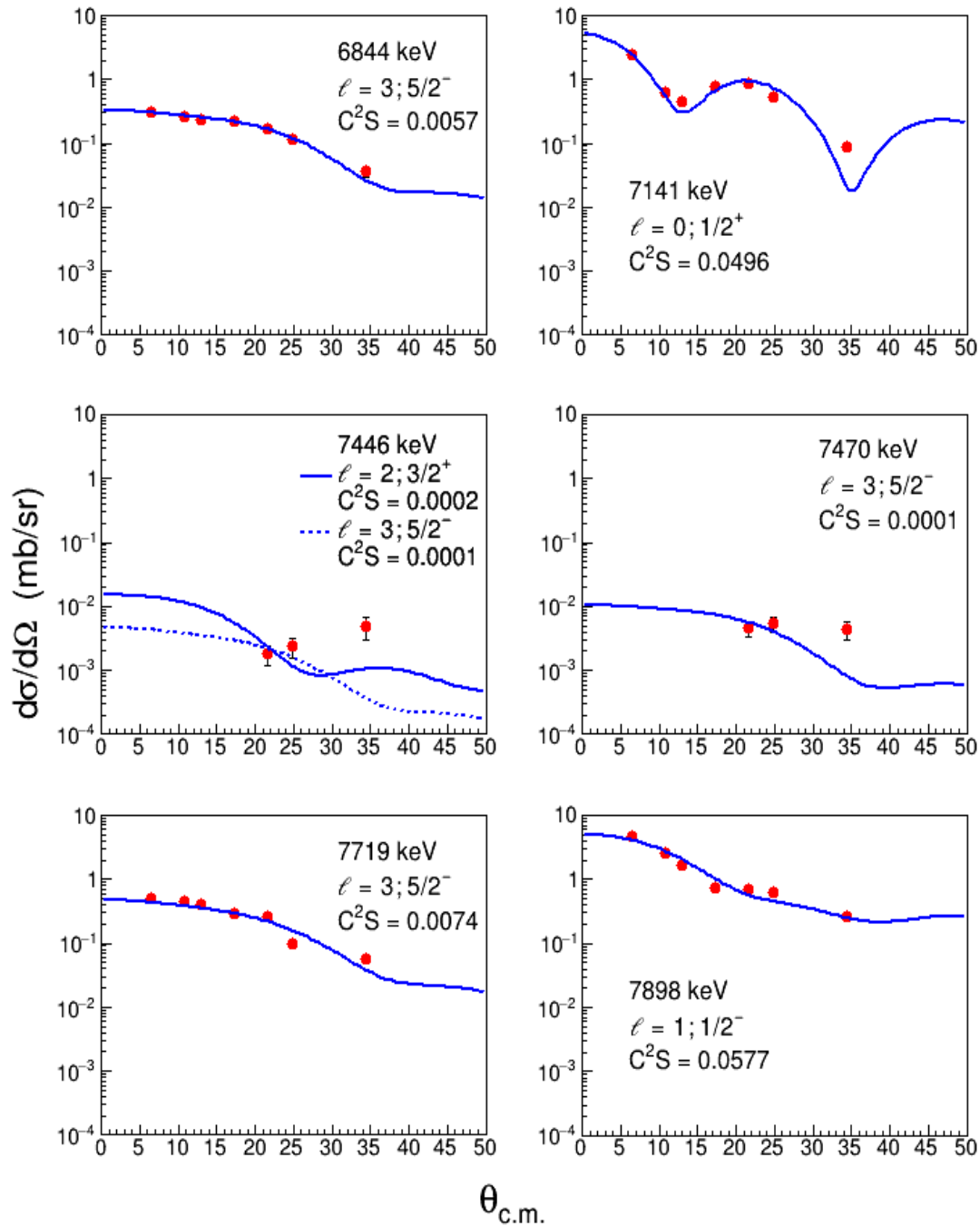
- Doublet at  $E_x = 7719 - 7737$  keV separated.

# Magnetic rigidity spectrum



- Doublet at  $E_x = 7719 - 7737$  keV separated.
- Levels at  $E_x = 7446$  and  $7470$  keV observed for  $\theta_{Q3D} \geq 20^\circ$ .

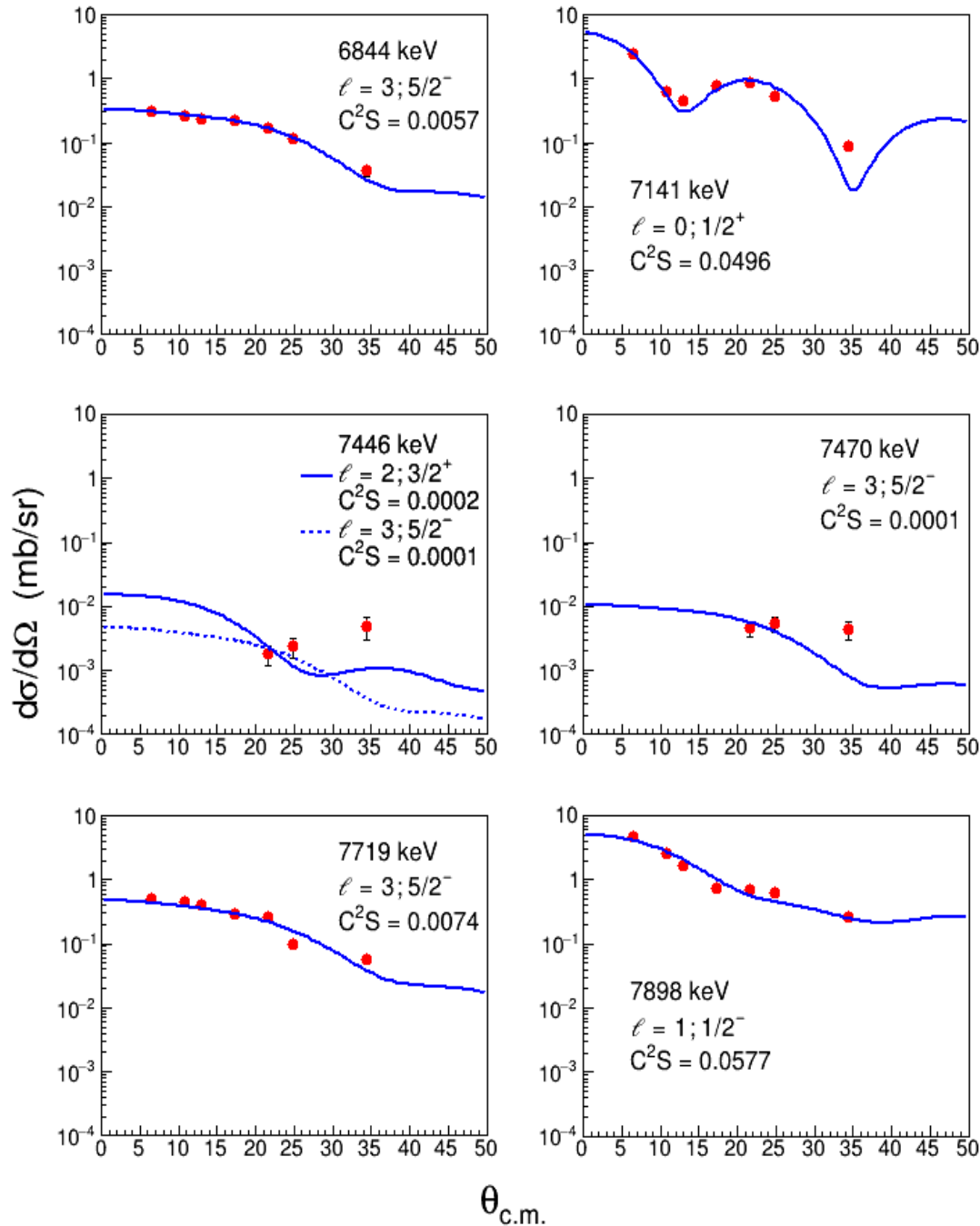
# Angular distributions



## Differential cross section

$$\frac{d\sigma}{d\Omega}(\theta_{c.m.})_{exp} = \frac{N_d(\theta_{c.m.})}{N_{beam}N_{target}\Delta\Omega_{c.m.}}$$

# Angular distributions



## Differential cross section

$$\frac{d\sigma}{d\Omega}(\theta_{c.m.})_{exp} = \frac{N_d(\theta_{c.m.})}{N_{beam}N_{target}\Delta\Omega_{c.m.}} = C^2S \frac{d\sigma}{d\Omega}(\theta_{c.m.})_{DWBA}$$

## Finite-Range DWBA calculations

→ performed with **FRESCO** code.

## Optical potentials

$^{30}\text{Si} + ^3\text{He}$ : Vernotte et al (1982)

$^{31}\text{P} + d$ : Daehnick, (1980)

## Binding Potentials

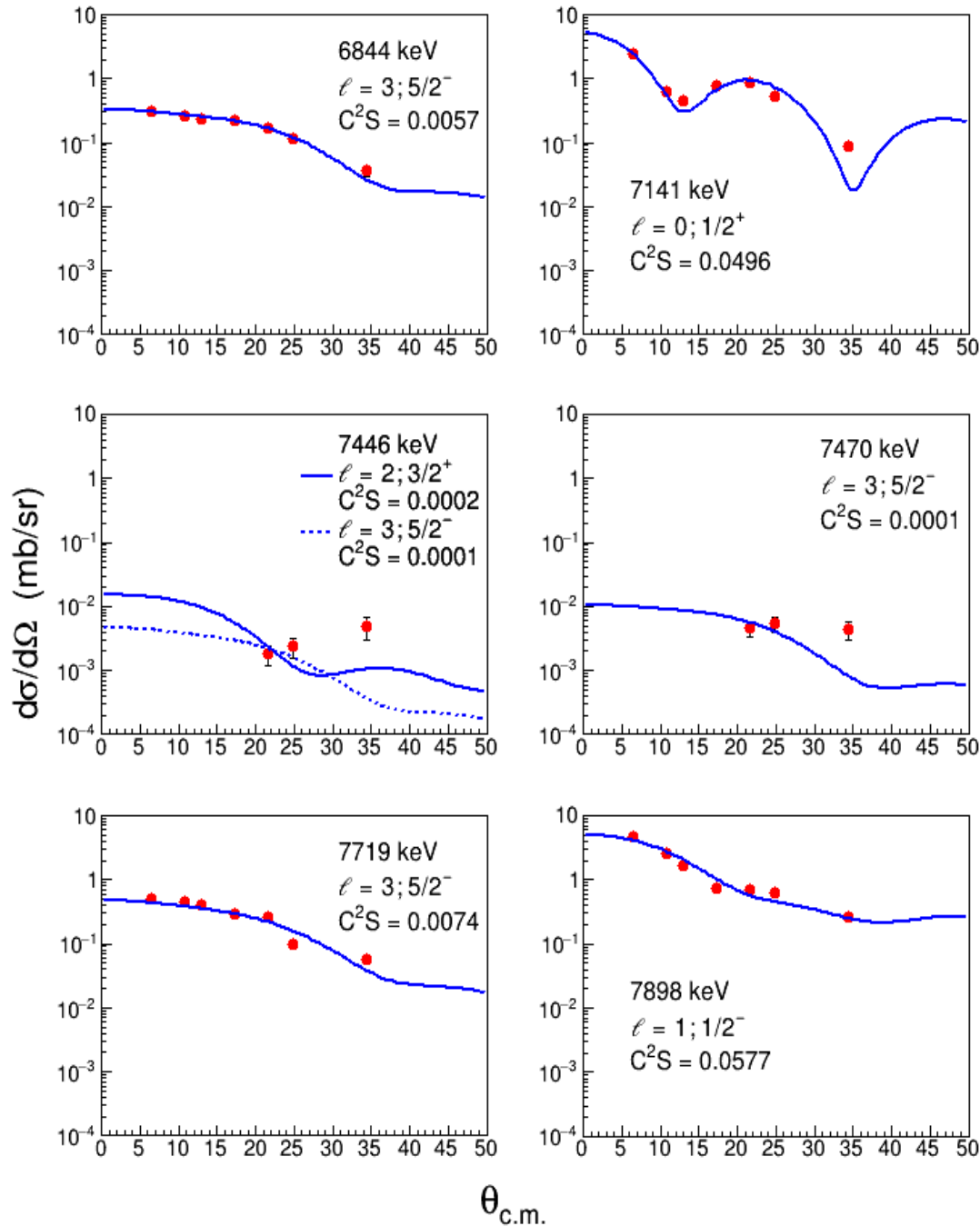
$^{30}\text{Si} + p$ : Wood-Saxon, volume + Spin-Orbit

$\langle ^3\text{He} | d+p \rangle$  overlap: GFMC Brida (2011)

→  $C^2S$  extrapolated to correct unbound energy



# Angular distributions



## Differential cross section

$$\frac{d\sigma}{d\Omega}(\theta_{c.m.})_{exp} = \frac{N_d(\theta_{c.m.})}{N_{beam}N_{target}\Delta\Omega_{c.m.}} = C^2S \frac{d\sigma}{d\Omega}(\theta_{c.m.})_{DWBA}$$

## Finite-Range DWBA calculations

→ performed with **FRESCO** code.

## Optical potentials

$^{30}\text{Si} + ^3\text{He}$ : Vernotte et al (1982)

$^{31}\text{P} + d$ : Daehnick, (1980)

## Binding Potentials

$^{30}\text{Si} + p$ : Wood-Saxon, volume + Spin-Orbit

$\langle ^3\text{He} | d + p \rangle$  overlap: GFMC Brida (2011)

→  $C^2S$  extrapolated to correct unbound energy

$$\Gamma_p \propto C^2S |R(r)|^2 \quad r = 7fm$$

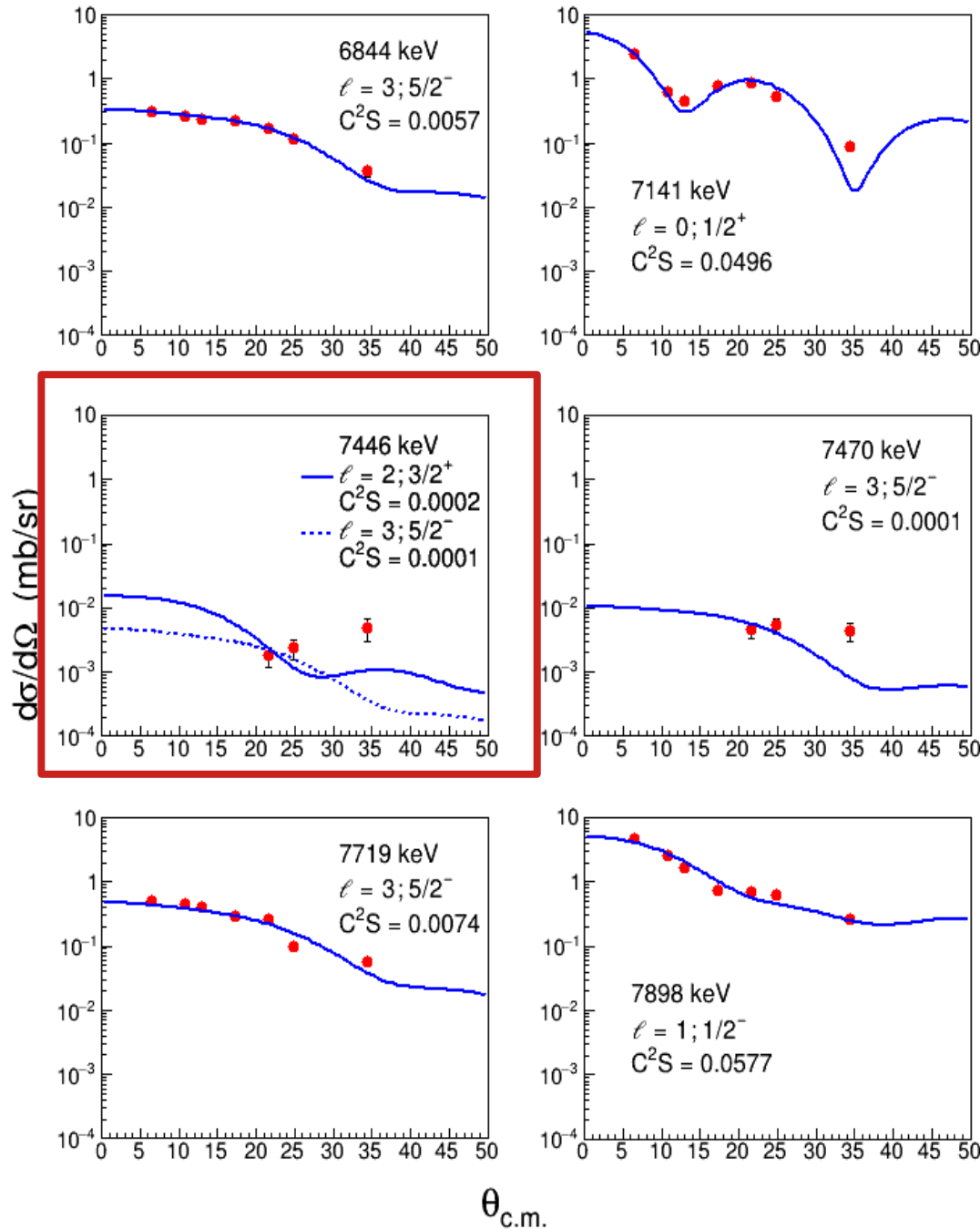
## Radial wave-function calculation

→ performed with **DWUCK4** code

Vincent & Fortune (1970) procedure

- $\Gamma_p$  uncertainties ~ 30% (from optical pot.)

# Angular distributions



## Differential cross section

$$\frac{d\sigma}{d\Omega}(\theta_{c.m.})_{exp} = \frac{N_d(\theta_{c.m.})}{N_{beam}N_{target}\Delta\Omega_{c.m.}} = C^2S \frac{d\sigma}{d\Omega}(\theta_{c.m.})_{DWBA}$$

## Finite-Range DWBA calculations

→ performed with **FRESCO** code.

## Optical potentials

$^{30}\text{Si} + ^3\text{He}$ : Vernotte et al (1982)

$^{31}\text{P} + d$ : Daehnick, (1980)

## Binding Potentials

$^{30}\text{Si} + p$ : Wood-Saxon, volume + Spin-Orbit

$\langle ^3\text{He} | d + p \rangle$  overlap: GFMC Brida (2011)

→  $C^2S$  extrapolated to correct unbound energy

$$\Gamma_p \propto C^2S |R(r)|^2 \quad r = 7fm$$

## Radial wave-function calculation

→ performed with **DWUCK4** code

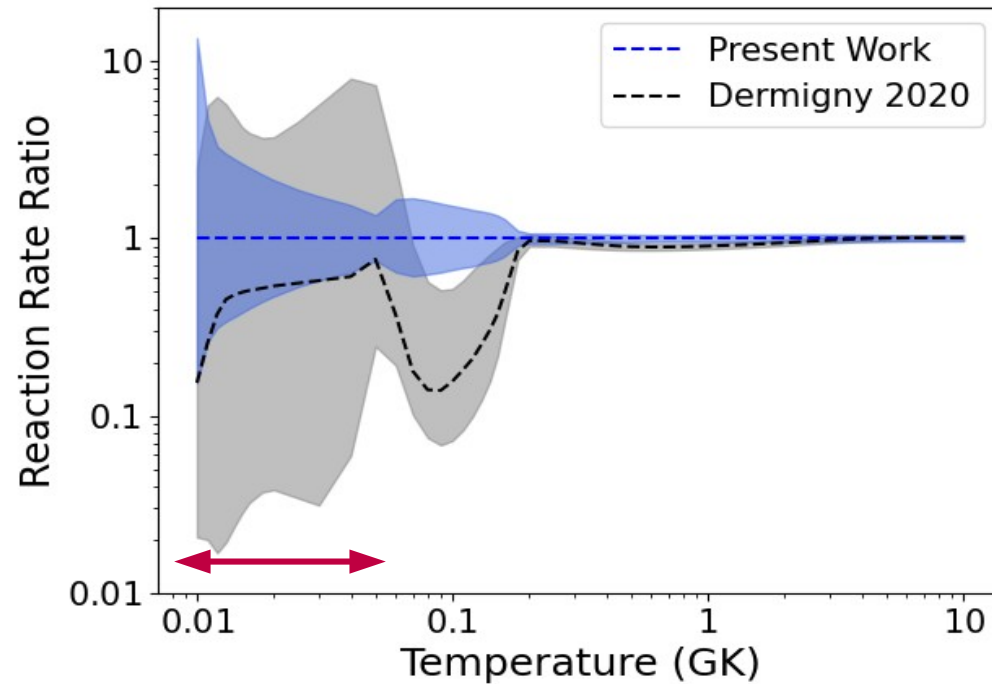
Vincent & Fortune (1970) procedure

- $\Gamma_p$  uncertainties ~ 30% (from optical pot.)



# $^{30}\text{Si}(p,\gamma)^{31}\text{P}$ Reaction Rate

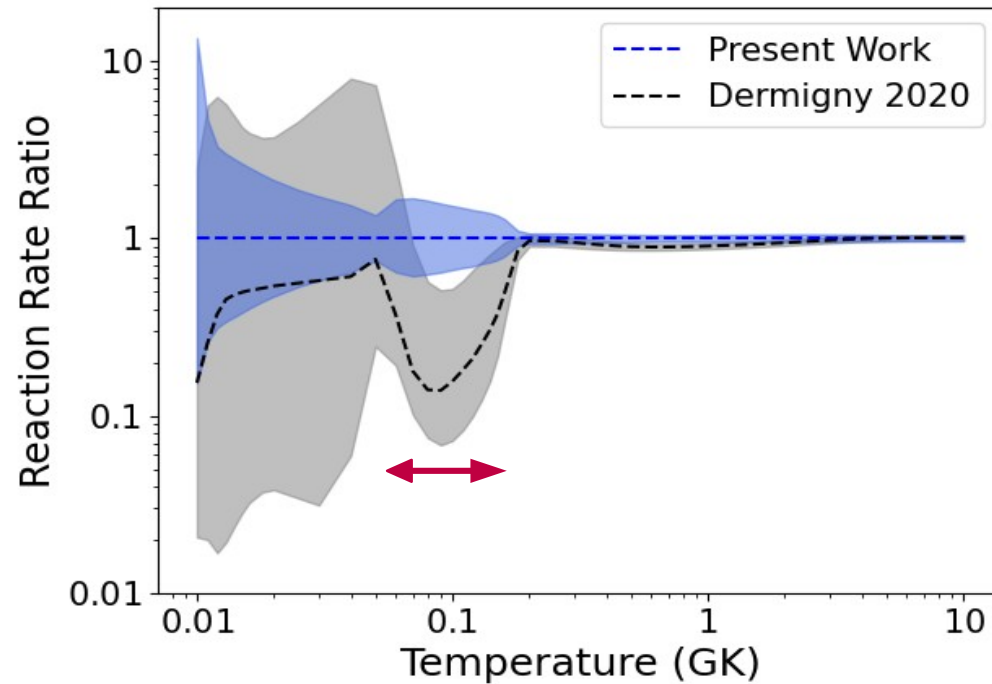
- Monte Carlo calculations using **RatesMC**.
- 68% uncertainty bands (log-normal distribution)



- Determination of C<sup>2</sup>S for  $E_r = 19$  keV,  $E_r = 51$  keV and  $E_r = 170$  keV (previously upper limits)

# $^{30}\text{Si}(p,\gamma)^{31}\text{P}$ Reaction Rate

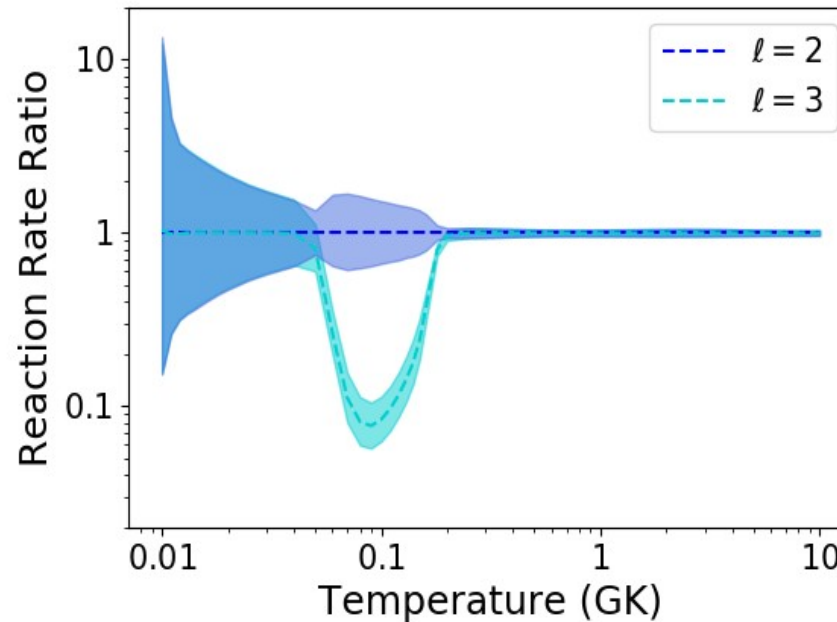
- Monte Carlo calculations using **RatesMC**.
- 68% uncertainty bands (log-normal distribution)



- Determination of  $\text{C}^2\text{S}$  for  $E_r = 19$  keV,  $E_r = 51$  keV and  $E_r = 170$  keV (previously upper limits)
- Observation of the  $E_r = 149$  keV  $\rightarrow$  **key resonance** in  $T = 100\text{-}200$  MK

# $^{30}\text{Si}(p,\gamma)^{31}\text{P}$ Reaction Rate

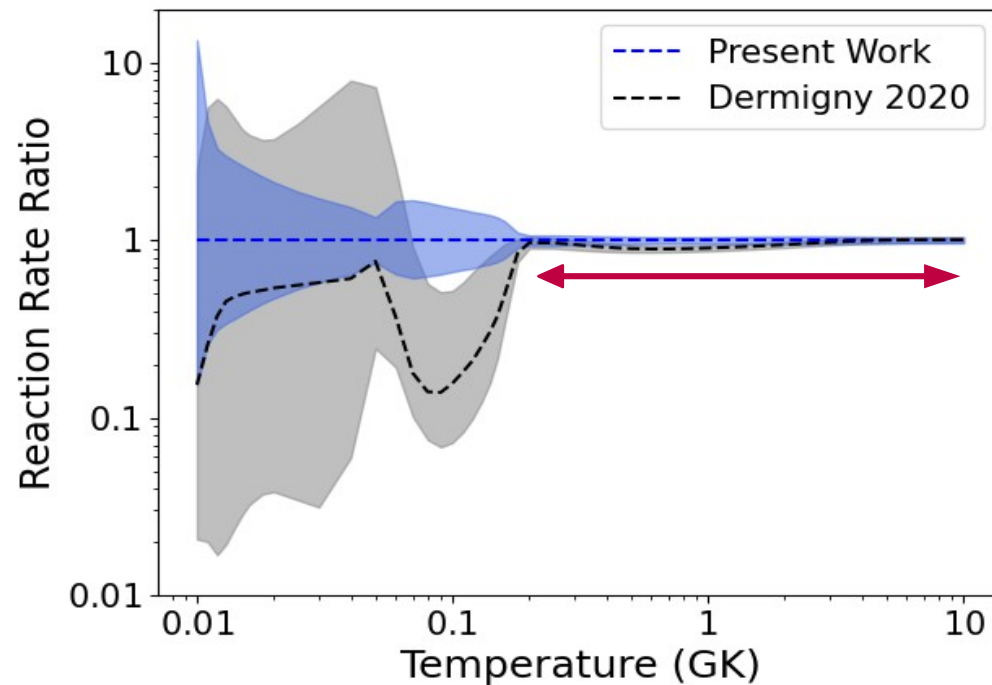
- Monte Carlo calculations using **RatesMC**.
- 68% uncertainty bands (log-normal distribution)



- Determination of C<sup>2</sup>S for  $E_r = 19$  keV,  $E_r = 51$  keV and  $E_r = 170$  keV (previously upper limits)
- Observation of the  $E_r = 149$  keV → **key resonance** in  $T = 100\text{-}200$  MK
  - $\ell = 2$  or  $\ell = 3$ , induces a factor of 10 difference in the reaction rate
  - **spin/parity have to be better constrained!**

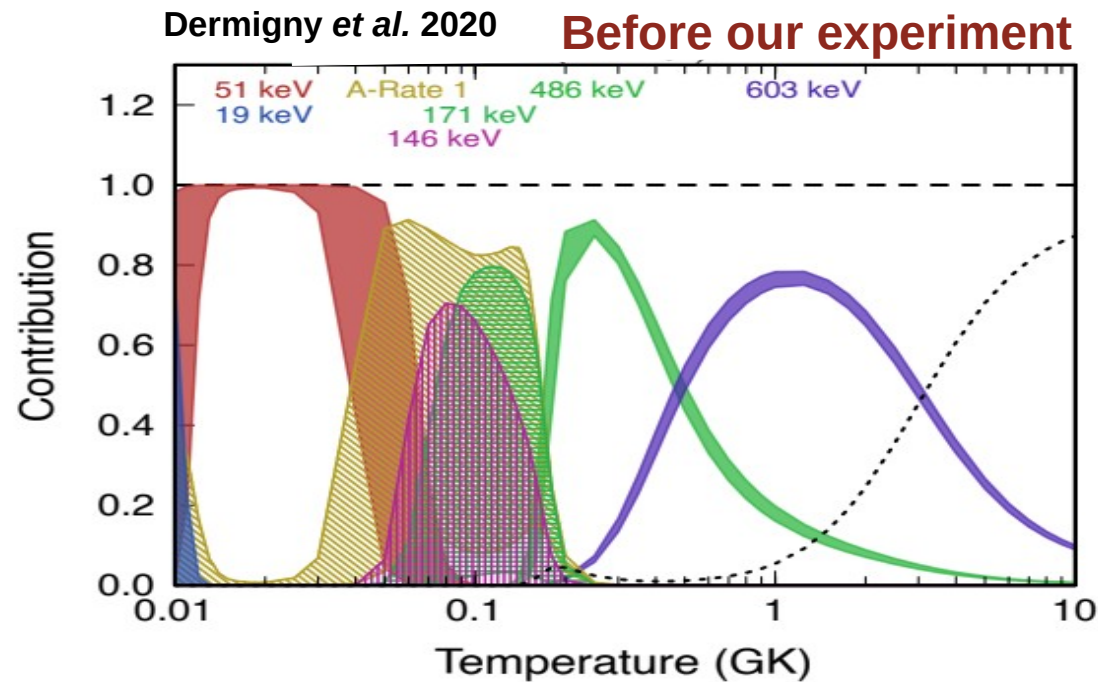
# $^{30}\text{Si}(p,\gamma)^{31}\text{P}$ Reaction Rate

- Monte Carlo calculations using **RatesMC**.
- 68% uncertainty bands (log-normal distribution)



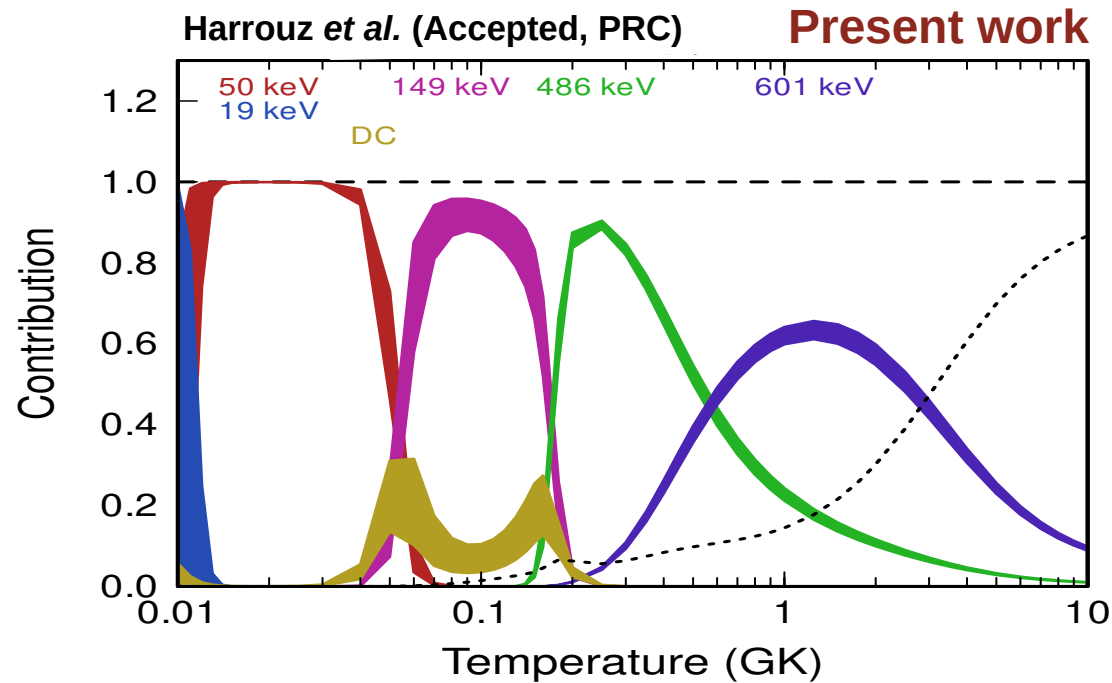
- Determination of C<sup>2</sup>S for  $E_r = 19$  keV,  $E_r = 51$  keV and  $E_r = 170$  keV (previously upper limits)
- Observation of the  $E_r = 149$  keV → **key resonance** in  $T = 100$ -200 MK
- →  $\ell = 2$  or  $\ell = 3$ , induces a factor of 10 difference in the reaction rate  
→ **spin/parity have to be better constrained!**
- $E_r = 418$  - 440 keV doublet resolved →  $E_r = 418$  keV has  $\ell=3$ , negligible contribution to the reaction rate, in agreement with direct measurements (*Dermigny et al. 2020*)
- $E_r = 486$  keV: good agreement for strength values (within 30%) with direct measurements.

# $^{30}\text{Si}(p,\gamma)^{31}\text{P}$ Reaction Rate




- Determination of C<sup>2</sup>S for  $E_r = 19$  keV,  $E_r = 51$  keV and  $E_r = 170$  keV (previously upper limits)
- Observation of the  $E_r = 149$  keV → **key resonance** in  $T = 100$ -200 MK
- →  $\ell = 2$  or  $\ell = 3$ , induces a factor of 10 difference in the reaction rate  
→ **spin/parity have to be better constrained!**
- $E_r = 418 - 440$  keV doublet resolved →  $E_r = 418$  keV has  $\ell=3$ , negligible contribution to the reaction rate, in agreement with direct measurements (*Dermigny et al. 2020*)
- $E_r = 486$  keV: good agreement for strength values (within 30%) with direct measurements.

# $^{30}\text{Si}(p,\gamma)^{31}\text{P}$ Reaction Rate



- Determination of C<sup>2</sup>S for  $E_r = 19$  keV,  $E_r = 51$  keV and  $E_r = 170$  keV (previously upper limits)
- Observation of the  $E_r = 149$  keV → **key resonance** in  $T = 100$ -200 MK
- →  $\ell = 2$  or  $\ell = 3$ , induces a factor of 10 difference in the reaction rate  
→ **spin/parity have to be better constrained!**
- $E_r = 418 - 440$  keV doublet resolved →  $E_r = 418$  keV has  $\ell=3$ , negligible contribution to the reaction rate, in agreement with direct measurements (*Dermigny et al. 2020*)
- $E_r = 486$  keV: good agreement for strength values (within 30%) with direct measurements.

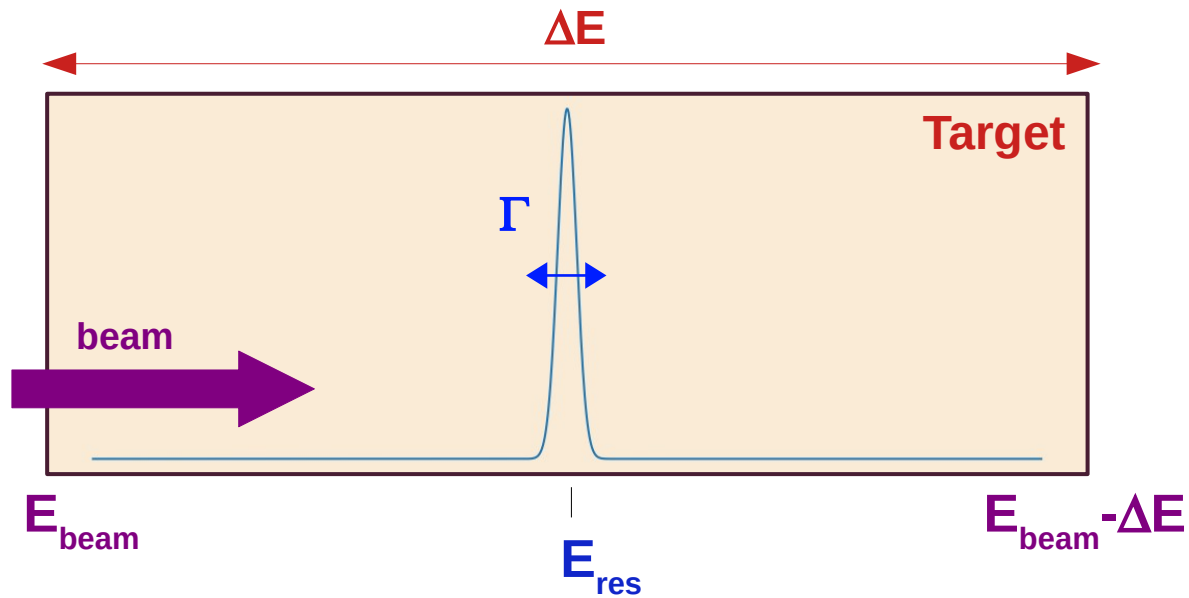


# Direct Measurement

$^{30}\text{Si}(\text{p},\gamma)^{31}\text{P}$



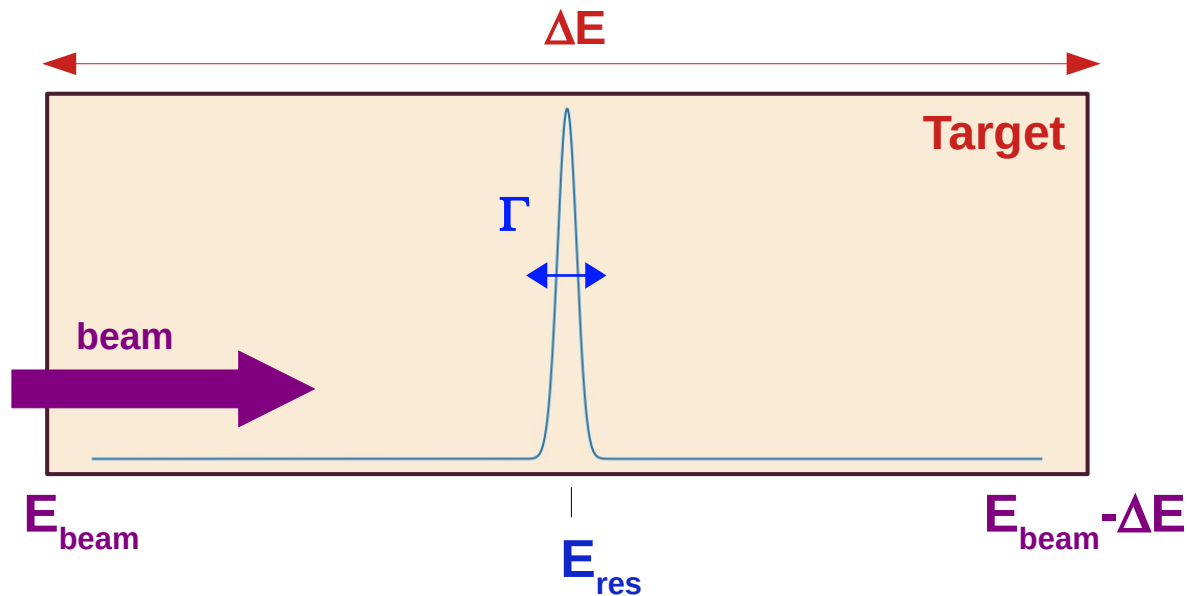
# Direct strength measurement



Yield :

$$Y = \frac{N_{\text{Reactions}}}{N_{\text{beam}}}$$

# Direct strength measurement

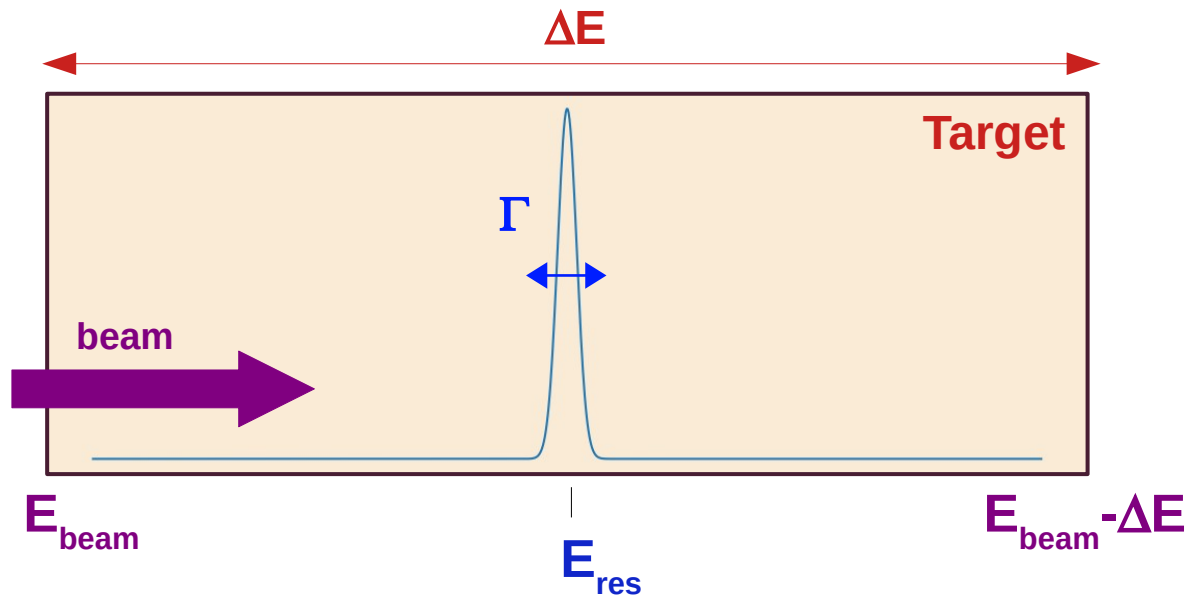


Yield : 
$$Y = \frac{N_{\text{Reactions}}}{N_{\text{beam}}}$$

- If  $\Gamma \ll \Delta E$  (thick target)

$$Y = \frac{\lambda_r^2}{2} \frac{m_b + m_t}{m_t} \frac{\omega \gamma}{\epsilon_r}$$

# Direct strength measurement

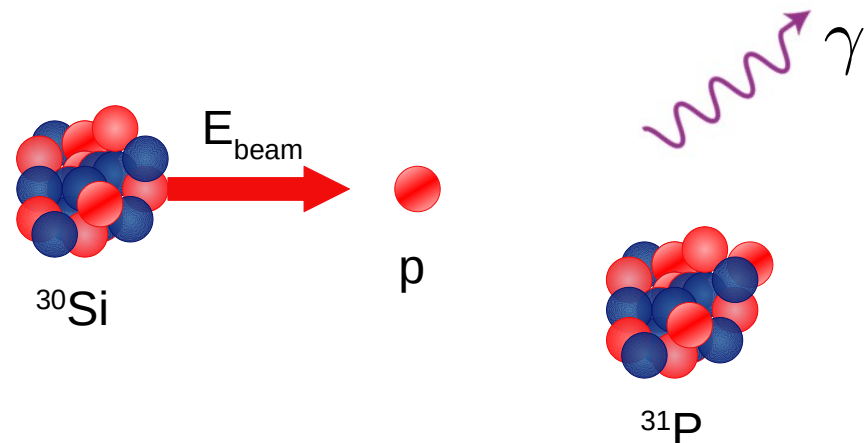


Yield : 
$$Y = \frac{N_{\text{Reactions}}}{N_{\text{beam}}}$$

- If  $\Gamma \ll \Delta E$  (thick target)

$$Y = \frac{\lambda_r^2}{2} \frac{m_b + m_t}{m_t} \frac{\omega \gamma}{\epsilon_r}$$

- Reaction in **inverse kinematics**  
→ Detection of recoils  
in **coincidence** with  $\gamma$ -ray



\_\_\_\_\_



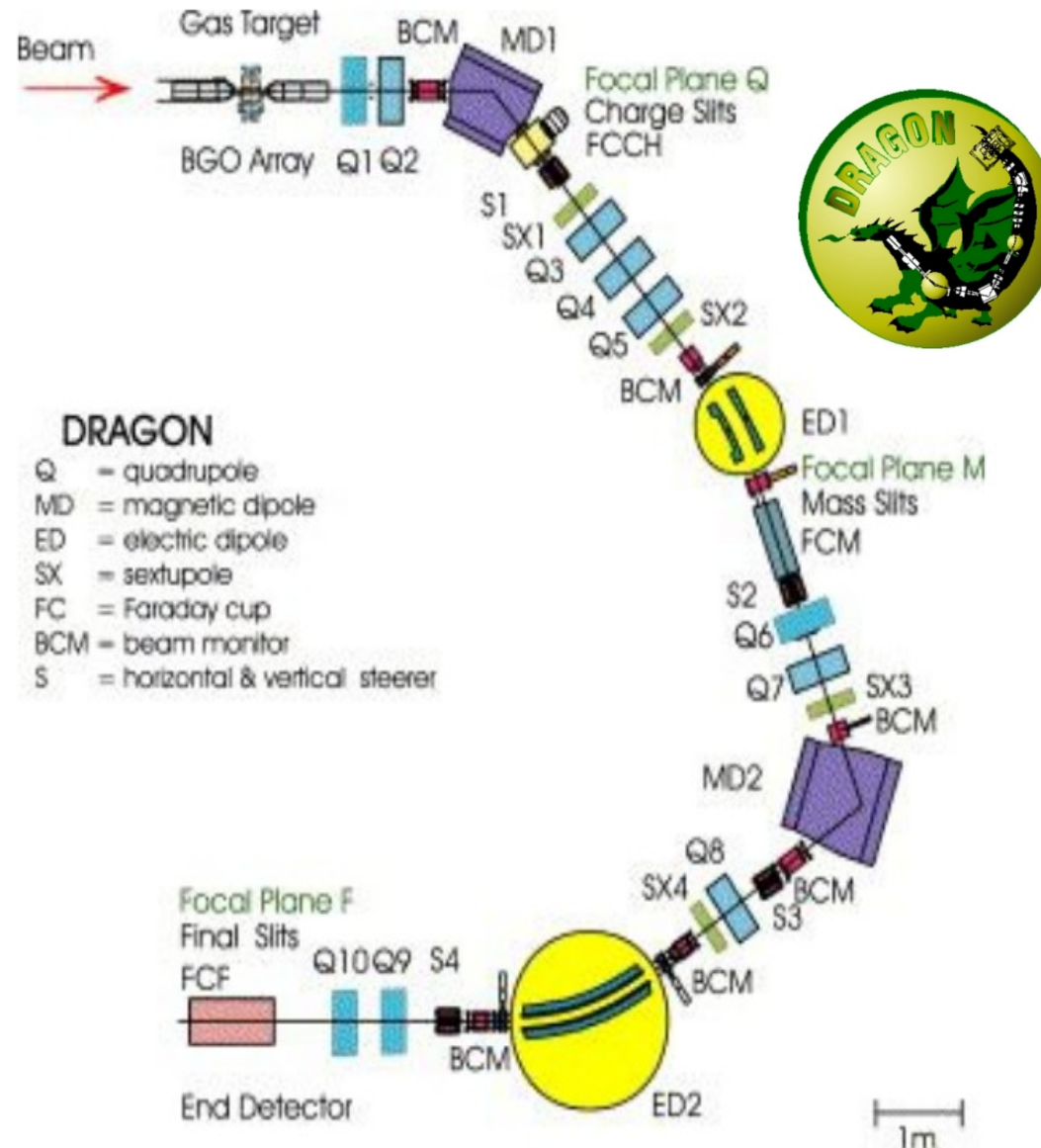
# The **D**etector of **R**ecoils **A**nd **G**ammas **O**f **N**uclear reactions.

Designed to measure the rates of nuclear reactions important in astrophysics ( $p,\gamma$ ) and ( $\alpha,\gamma$ )

## Beam suppression:

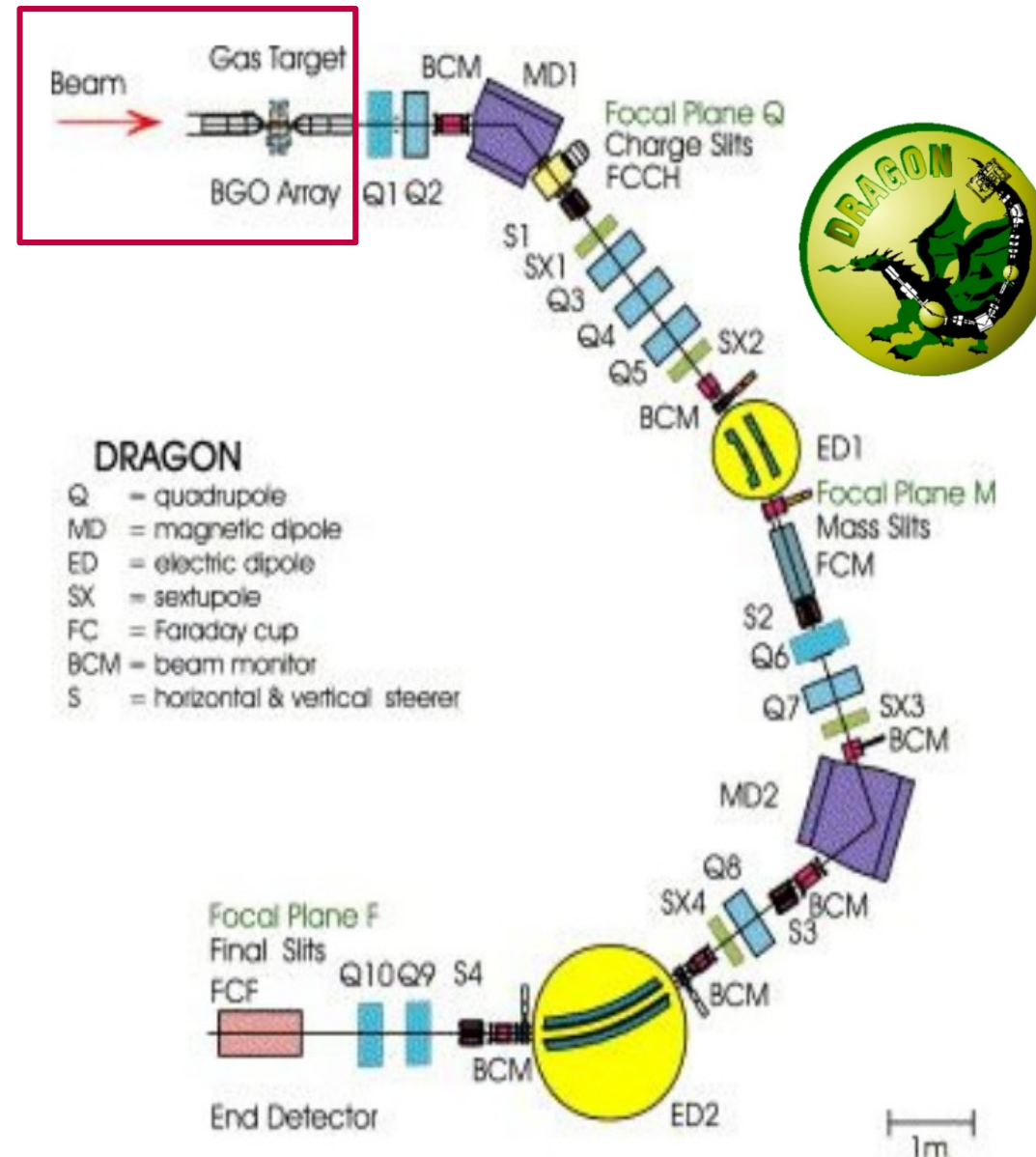
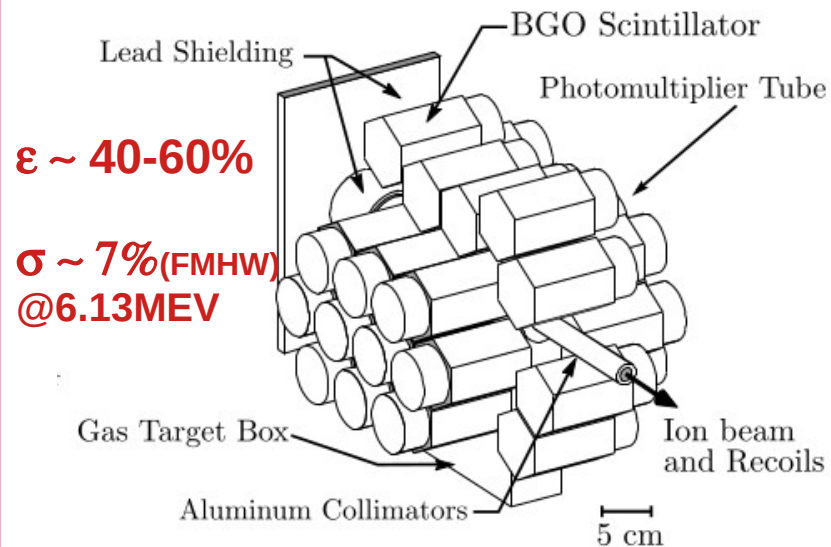
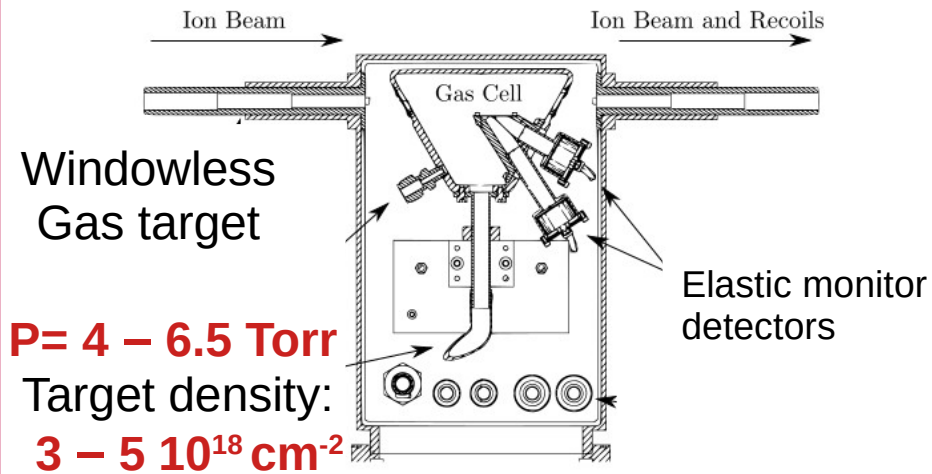
- Singles  $10^8 - 10^{13}$
- Coincidences  $10^{10} - 10^{16}$

Yield sensitivity down to  **$10^{-15}$**



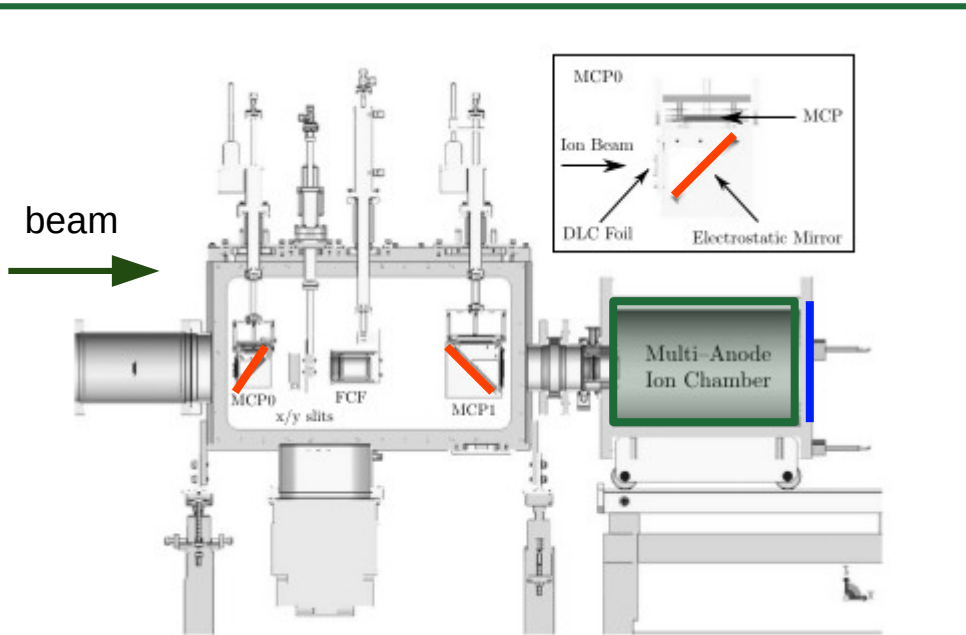
# DRAGON spectrometer

## DRAGON Head



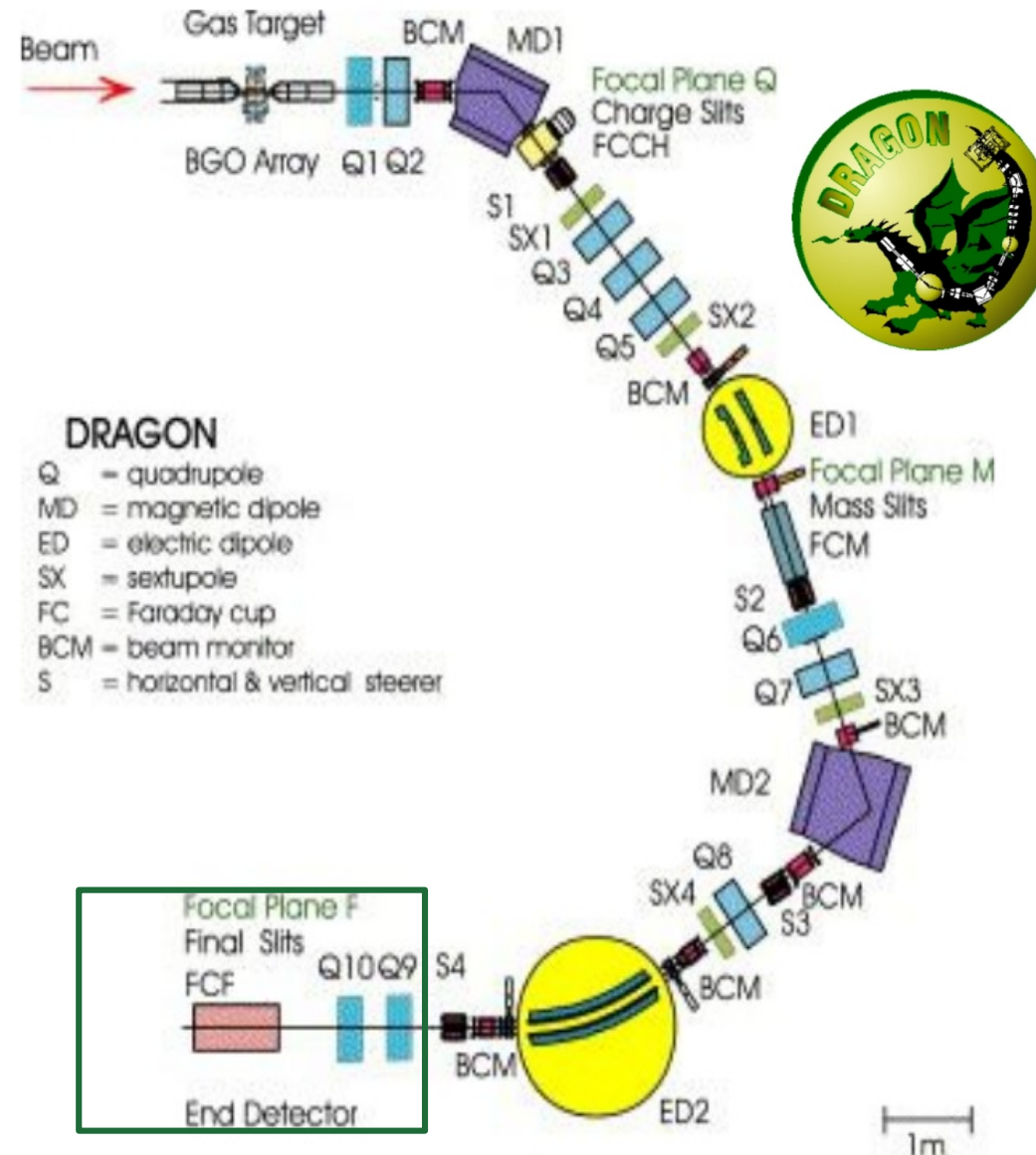
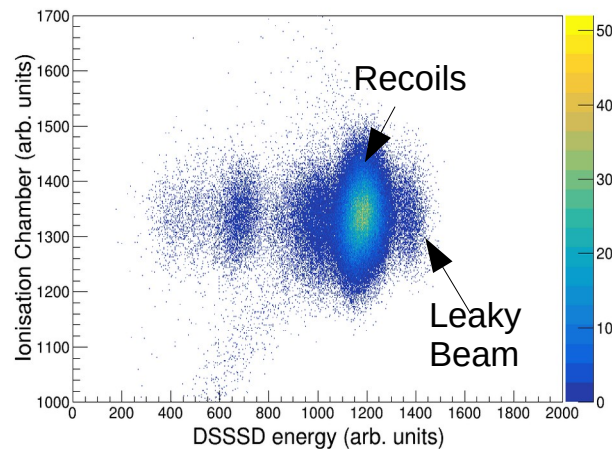
# DRAGON spectrometer

## DRAGON Tail



End detection equipped with:

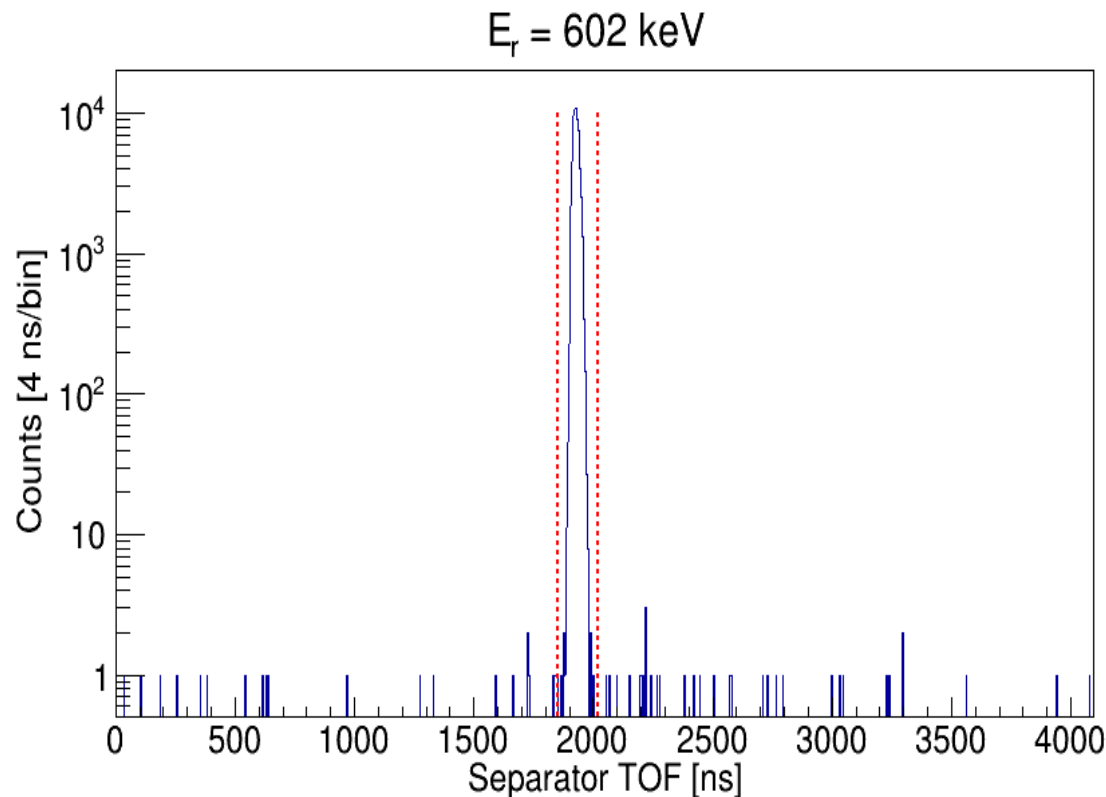
- **MCPs**
- **Ionisation chamber**
- **DSSSD**





# Ongoing Analysis

Measured resonances:  $E_r = 485, 555, 602, 752, 911$  and  $950$  keV



$$Y = \frac{N_R^{det}}{N_b \varepsilon_{DRA}}$$

$$\varepsilon_{DRA}^{coinc} = f_q \tau_{MCP} \varepsilon_{MCP} \varepsilon_{DSSSD} \varepsilon_\gamma \lambda_{coinc}$$

$f_q$  : Recoil charge state fraction

$\tau$  : Transmission efficiency

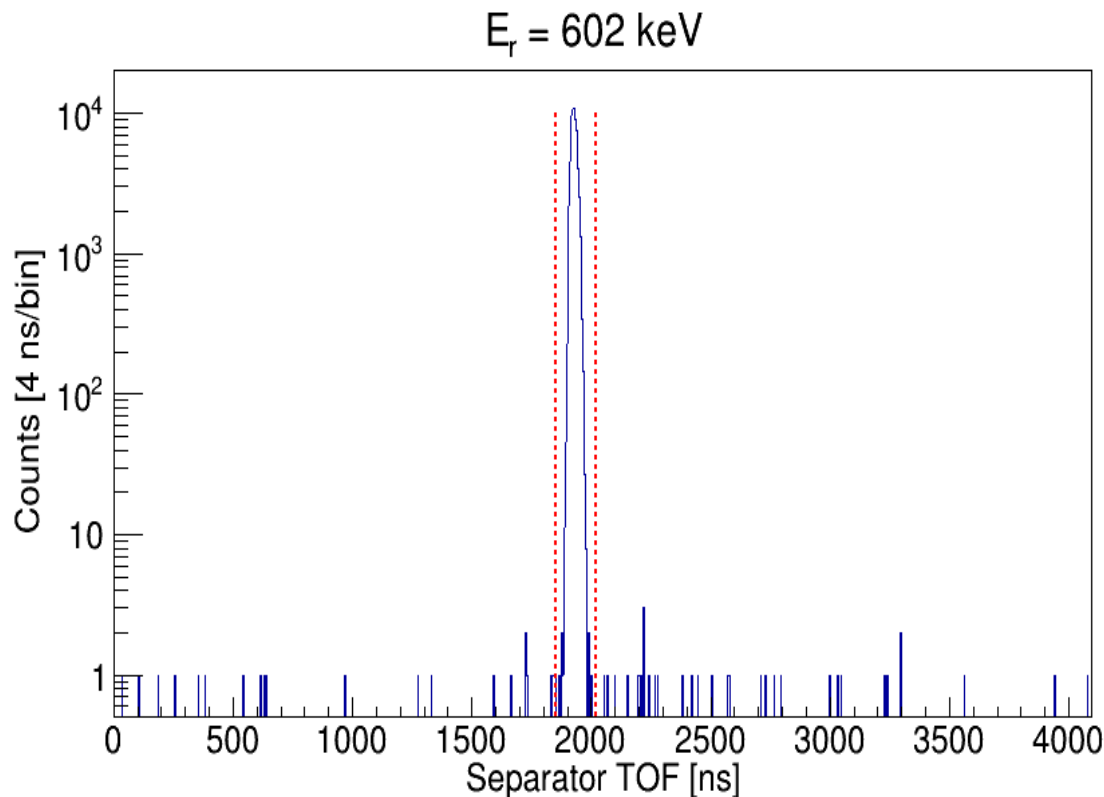
$\varepsilon$  : Detection efficiency

$\lambda$  : DAQ live time fraction



# Ongoing Analysis

Measured resonances:  $E_r = 485, 555, 602, 752, 911$  and  $950$  keV



$$Y = \frac{N_R^{det}}{N_b \varepsilon_{DRA}}$$

$$\varepsilon_{DRA}^{coinc} = f_q \tau_{MCP} \varepsilon_{MCP} \varepsilon_{DSSSD} \varepsilon_\gamma \lambda_{coinc}$$

$f_q$  : Recoil charge state fraction

$\tau$  : Transmission efficiency

$\varepsilon$  : Detection efficiency

$\lambda$  : DAQ live time fraction

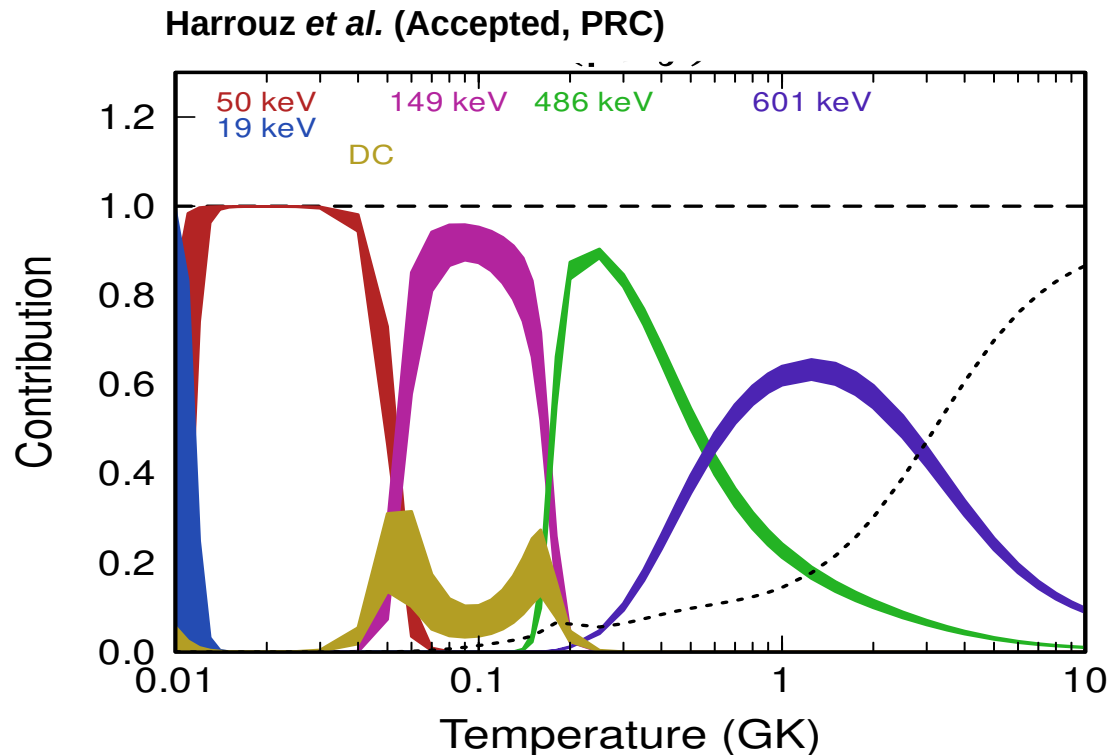
$$\varepsilon_{DRA}^{coinc} = 0.37 \ 0.88 \ 0.90 \ 0.93 \ 0.6 \ 0.72$$

$$\omega\gamma_{(\text{preliminary})} \approx 2 \text{ eV}$$

$$\omega\gamma_{(\text{literature})} = 1.95 \pm 0.10 \text{ eV}$$

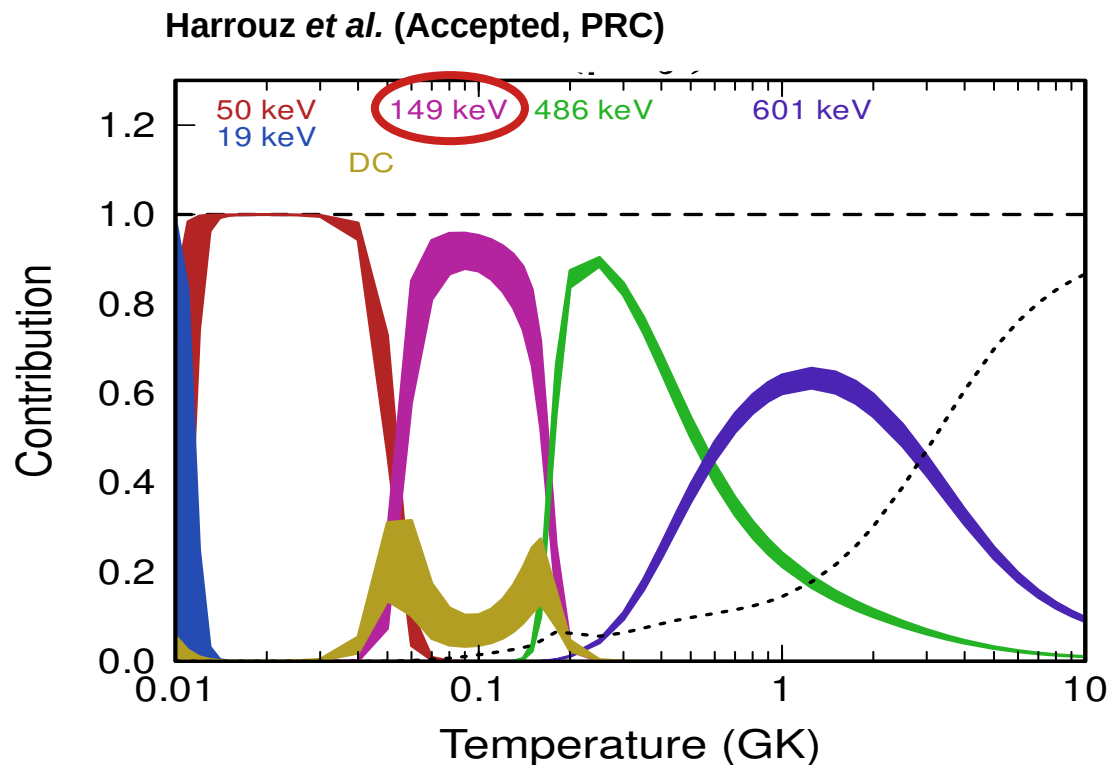
# Conclusion

- Extraction of spectroscopic information for the  $^{31}\text{P}$  nucleus between  $E_x = 6800 - 8100$  keV from the  $^{30}\text{Si}(^3\text{He},d)^{31}\text{P}$  reaction.
- Calculation of strengths for resonances up to  $E_r = 600$  keV.
- Improved determination of the  $^{30}\text{Si}(p,\gamma)^{31}\text{P}$  reaction rate.



# Conclusion

- Extraction of spectroscopic information for the  $^{31}\text{P}$  nucleus between  $E_x = 6800 - 8100$  keV from the  $^{30}\text{Si}(^3\text{He},d)^{31}\text{P}$  reaction.
- Calculation of strengths for resonances up to  $E_r = 600$  keV.
- Improved determination of the  $^{30}\text{Si}(p,\gamma)^{31}\text{P}$  reaction rate.
- Evincing the importance of key resonance at  $E_r = 149$  keV → **need to determine its spin/parity**

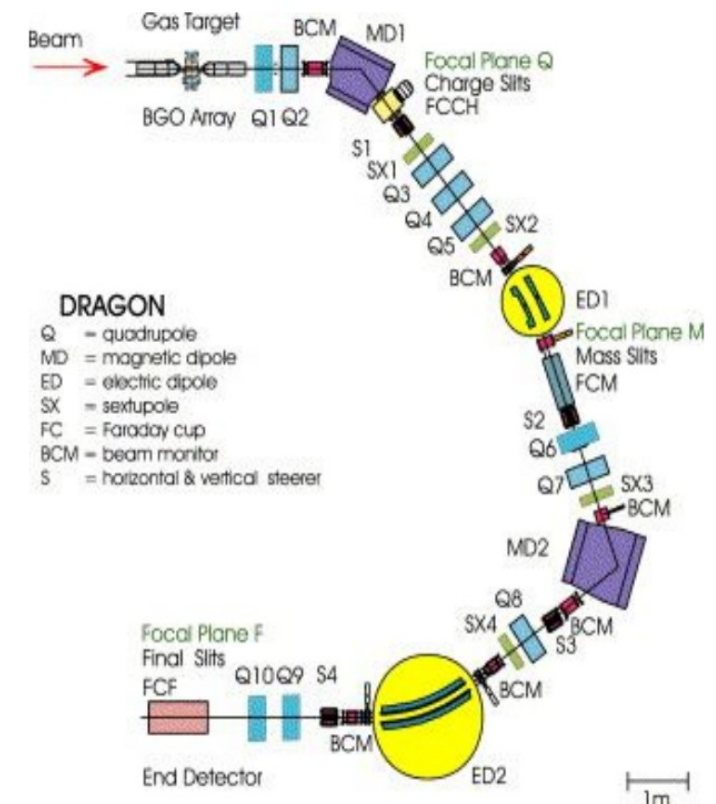


# Conclusion

- Extraction of spectroscopic information for the  $^{31}\text{P}$  nucleus between  $E_x = 6800 - 8100$  keV from the  $^{30}\text{Si}(^3\text{He}, d)^{31}\text{P}$  reaction.
- Calculation of strengths for resonances up to  $E_r = 600$  keV.
- Improved determination of the  $^{30}\text{Si}(p, \gamma)^{31}\text{P}$  reaction rate.
- Evincing the importance of key resonance at  $E_r = 149$  keV  $\rightarrow$  need to determine its spin/parity

## Perspectives

- Complete the analysis of the  $^{30}\text{Si}(p, \gamma)^{31}\text{P}$  reaction rate with the Recoil spectrometer **DRAGON**



# Conclusion

- Extraction of spectroscopic information for the  $^{31}\text{P}$  nucleus between  $E_x = 6800 - 8100$  keV from the  $^{30}\text{Si}(^3\text{He},d)^{31}\text{P}$  reaction.
- Calculation of strengths for resonances up to  $E_r = 600$  keV.
- Improved determination of the  $^{30}\text{Si}(p,\gamma)^{31}\text{P}$  reaction rate.
- Evincing the importance of key resonance at  $E_r = 149$  keV  $\rightarrow$  need to determine its spin/parity

## Perspectives

- Complete the analysis of the  $^{30}\text{Si}(p,\gamma)^{31}\text{P}$  reaction rate with the Recoil spectrometer **DRAGON**
- Investigate the impact of the new measurements on the temperature locus for constraining “the polluter” candidates in **Globular Clusters**.







M13

## Collaborators :

### Q3D

Philip Adsley ( <i>TA&amp;M</i> )	Anne Meyer ( <i>IJCLab</i> )
Beyhan Bastin ( <i>GANIL</i> )	Sara Palmerini ( <i>LNS</i> )
Thomas Fastermann ( <i>TUM</i> )	Gianluca Pizzone ( <i>LNS</i> )
Faïrouz Hammache ( <i>IJCLab</i> )	Stefano Romano ( <i>LNS</i> )
Ralf Hertenberger ( <i>TUM</i> )	Nicolas de Séréville ( <i>IJCLab</i> )
Marco La Cognata ( <i>LNS</i> )	Aurora Tumino ( <i>LNS</i> )
Livio Lamia ( <i>LNS</i> )	Hans-Friedrich Wirth ( <i>TUM</i> )
Richard Longlond ( <i>NCSU/TUNL</i> )	

### DRAGON

Philip Adsley ( <i>TA&amp;M</i> )	Athanasios Psaltis ( <i>TUD</i> )
Uwe Greif ( <i>CS Mines</i> )	Chris Ruiz ( <i>TRIUMF</i> )
Faïrouz Hammache ( <i>IJCLab</i> )	Nicolas de Séréville ( <i>IJCLab</i> )
Keerthi Jayamanna ( <i>TRIUMF</i> )	Sriteja Upadhyayula ( <i>TRIUMF</i> )
Spencer Kiy ( <i>TRIUMF</i> )	Matthew Williams ( <i>TRIUMF</i> )
Alison Laird ( <i>York</i> )	



# Thank you for your attention

## Collaborators :

### Q3D

Philip Adsley ( <i>TA&amp;M</i> )	Anne Meyer ( <i>IJCLab</i> )
Beyhan Bastin ( <i>GANIL</i> )	Sara Palmerini ( <i>LNS</i> )
Thomas Faermann ( <i>TUM</i> )	Gianluca Pizzone ( <i>LNS</i> )
Faïrouz Hammache ( <i>IJCLab</i> )	Stefano Romano ( <i>LNS</i> )
Ralf Hertenberger ( <i>TUM</i> )	Nicolas de Séréville ( <i>IJCLab</i> )
Marco La Cognata ( <i>LNS</i> )	Aurora Tumino ( <i>LNS</i> )
Livio Lamia ( <i>LNS</i> )	Hans-Friedrich Wirth ( <i>TUM</i> )
Richard Longlond ( <i>NCSU/TUNL</i> )	

### DRAGON

Philip Adsley ( <i>TA&amp;M</i> )	Athanasios Psaltis ( <i>TUD</i> )
Uwe Greif ( <i>CS Mines</i> )	Chris Ruiz ( <i>TRIUMF</i> )
Faïrouz Hammache ( <i>IJCLab</i> )	Nicolas de Séréville ( <i>IJCLab</i> )
Keerthi Jayamanna ( <i>TRIUMF</i> )	Sriteja Upadhyayula ( <i>TRIUMF</i> )
Spencer Kiy ( <i>TRIUMF</i> )	Matthew Williams ( <i>TRIUMF</i> )
Alison Laird ( <i>York</i> )	





# Backup

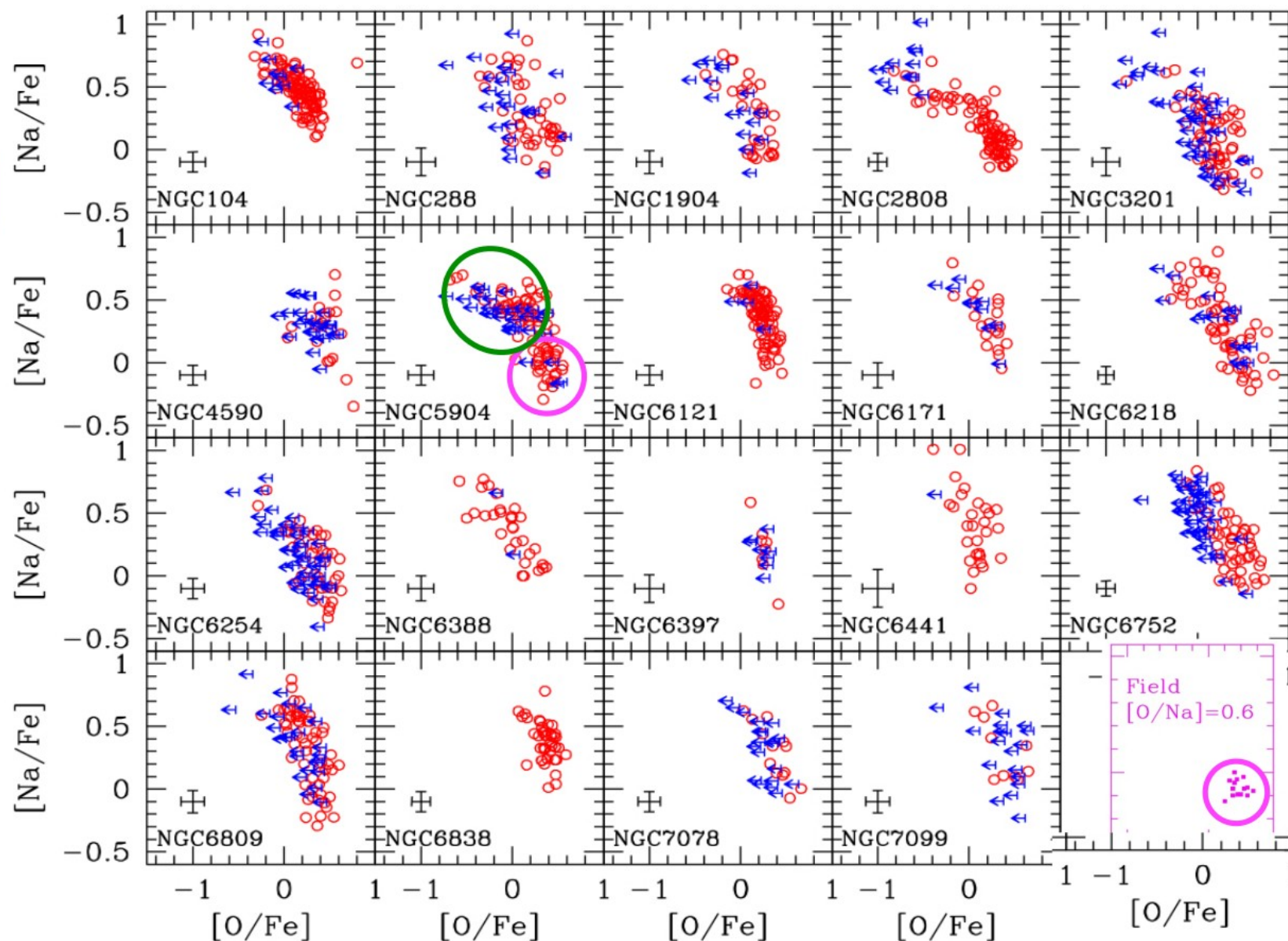
# GC anomalies

1<sup>st</sup> population

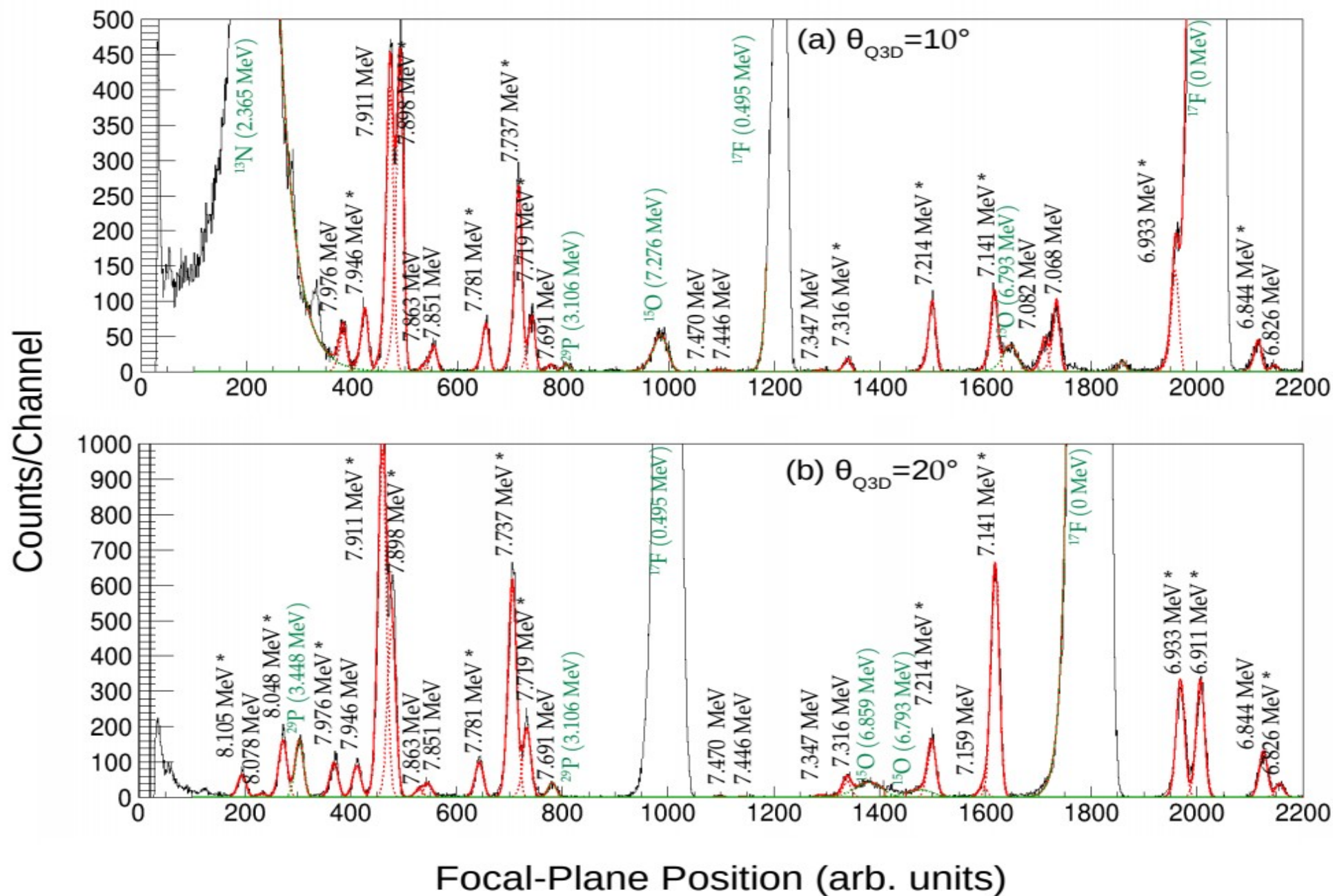
$\sim 30 \pm 7 \%$

2<sup>d</sup> population

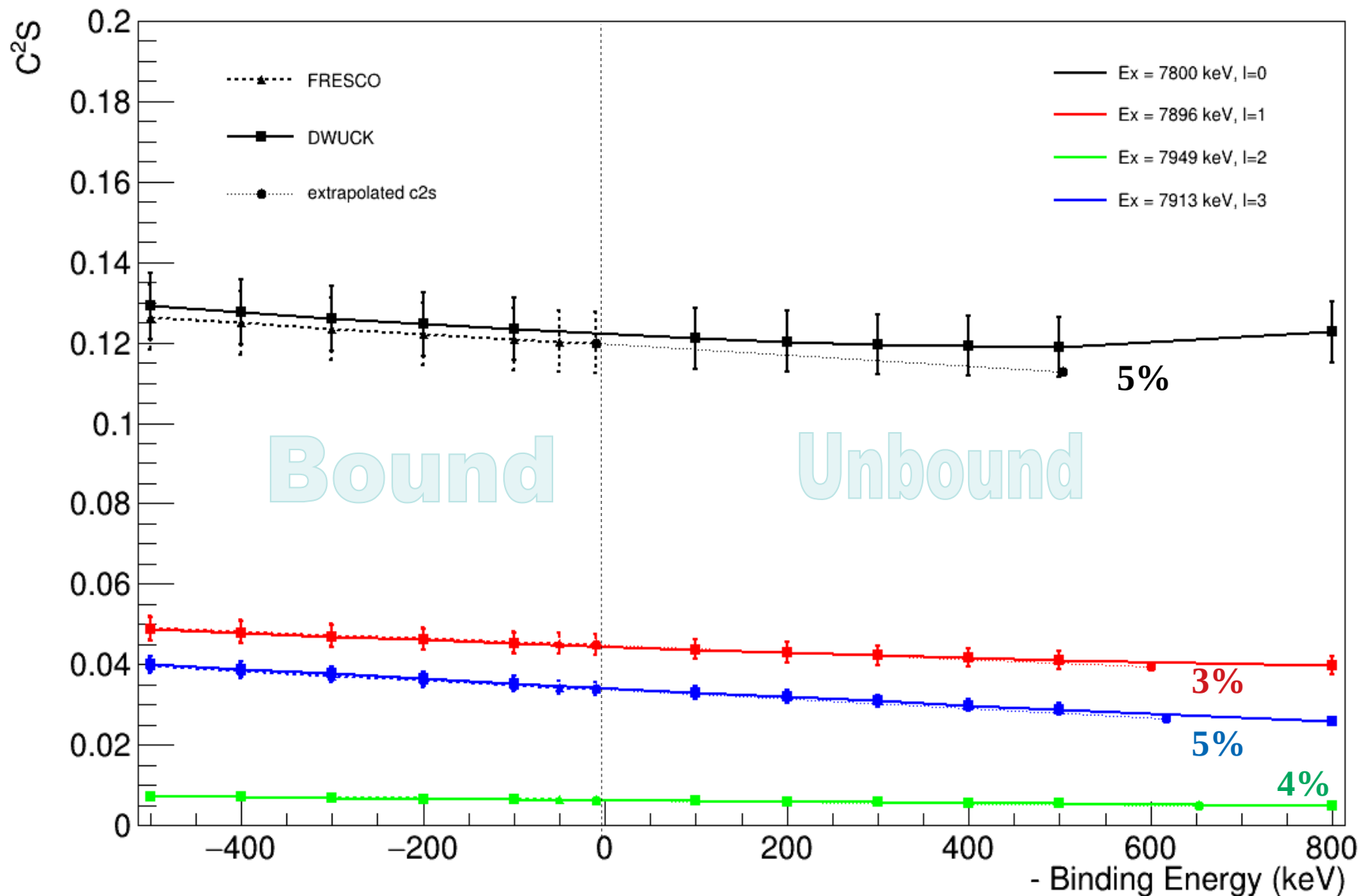
$\sim 70 \pm 7 \%$



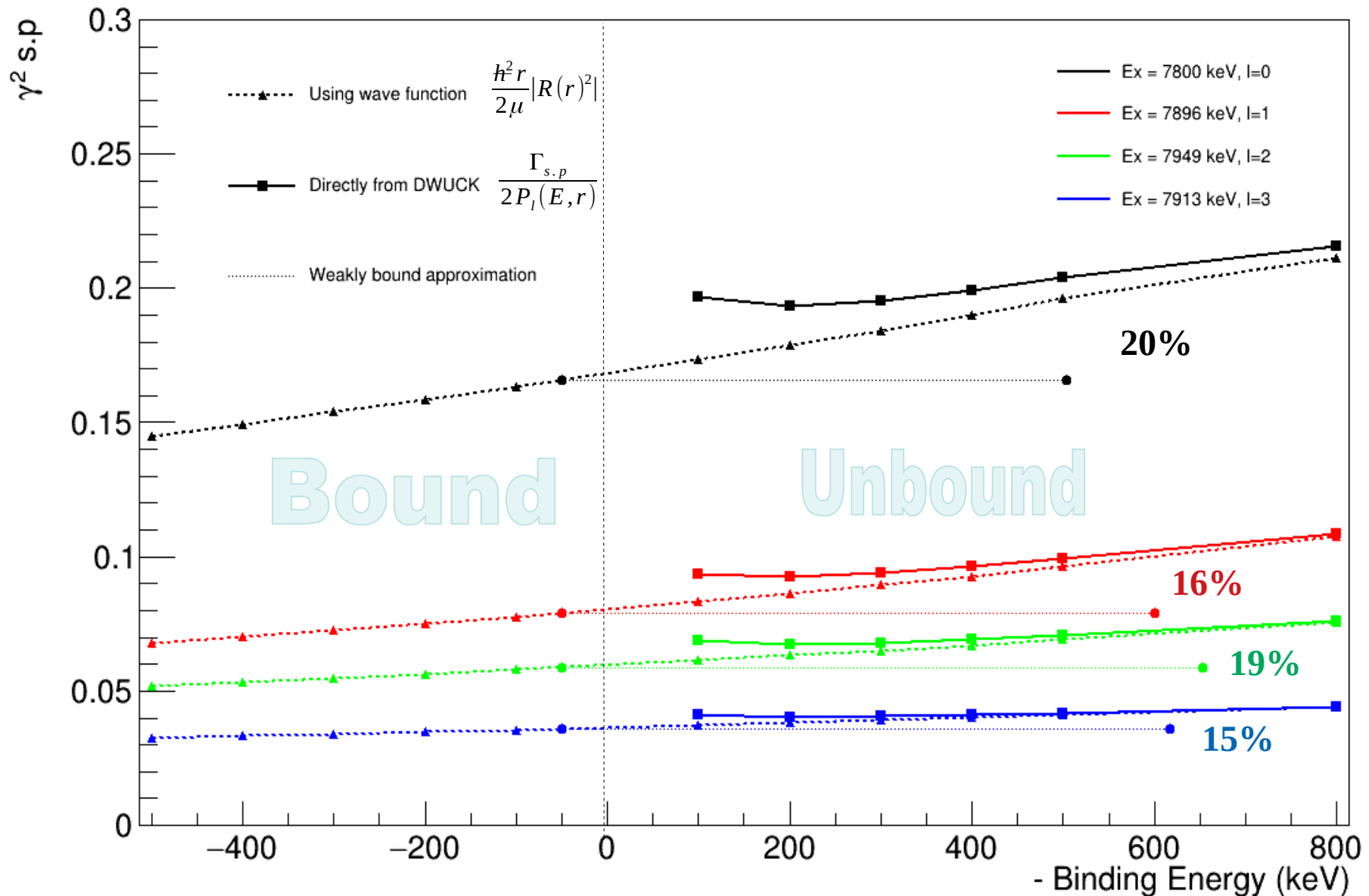
# Spectra



# Spectroscopic factor



# Reduced Partial Width s.p (DWUCK4)

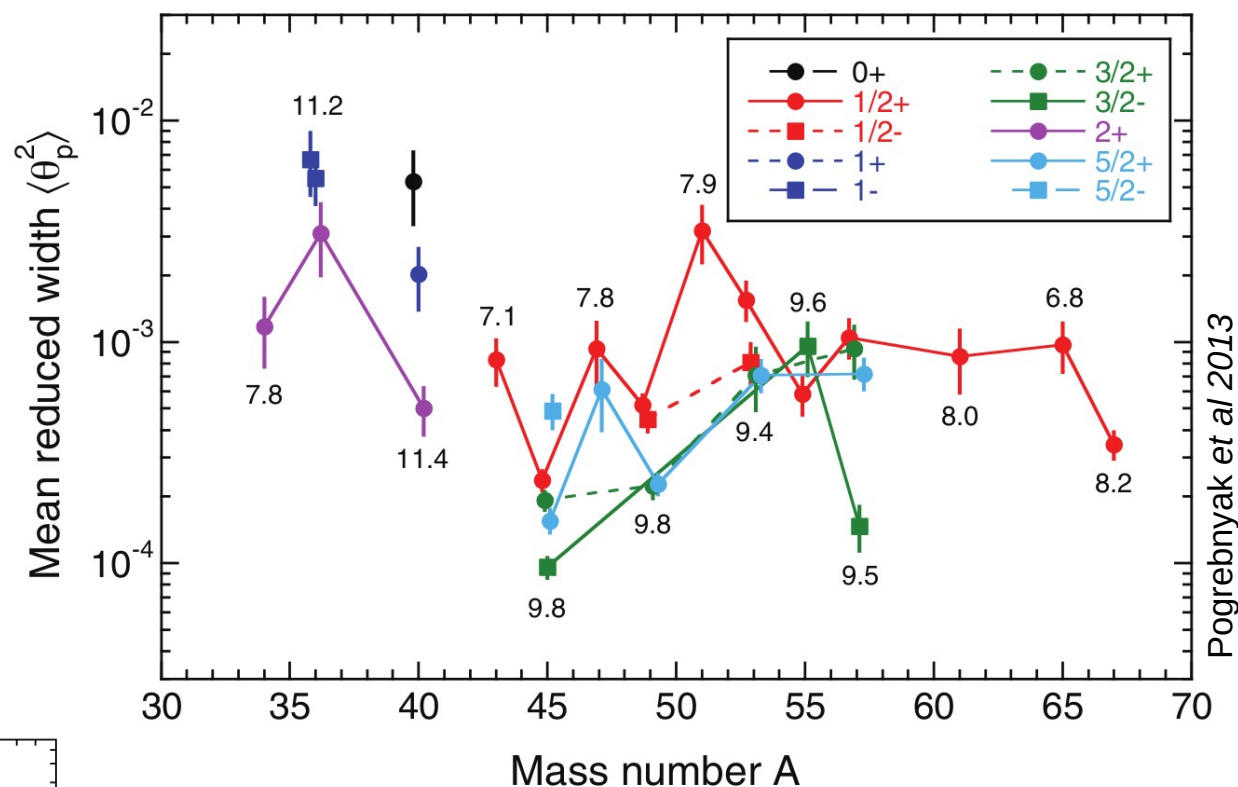


# Reduced width

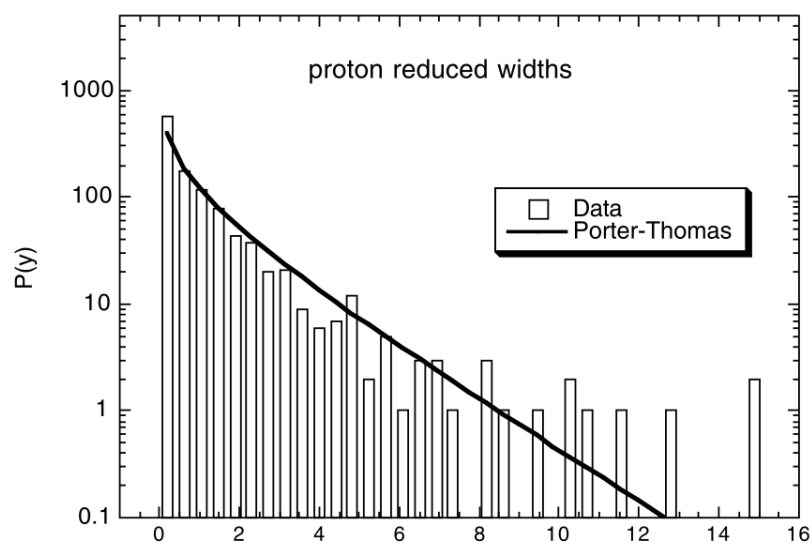
$$\Gamma_p = \theta_p^2 \Gamma_{Wigner}$$

In Dermigny 2020 :

$$\langle \theta^2 \rangle = 0.0003$$



Pogrebnyak et al 2013



Longland et al 2010

$$f(\theta^2) = \frac{c}{\sqrt{\theta^2}} e^{-\theta^2/(2\langle \theta^2 \rangle)}$$



# Partial widths uncertainties

- Uncertainties comes from optical potentials for entrance/exit channels and geometry of binding potential. → 20 – 30% (Keeley *et al.* 2013)
- Use same wave function coming from DWBA analysis.

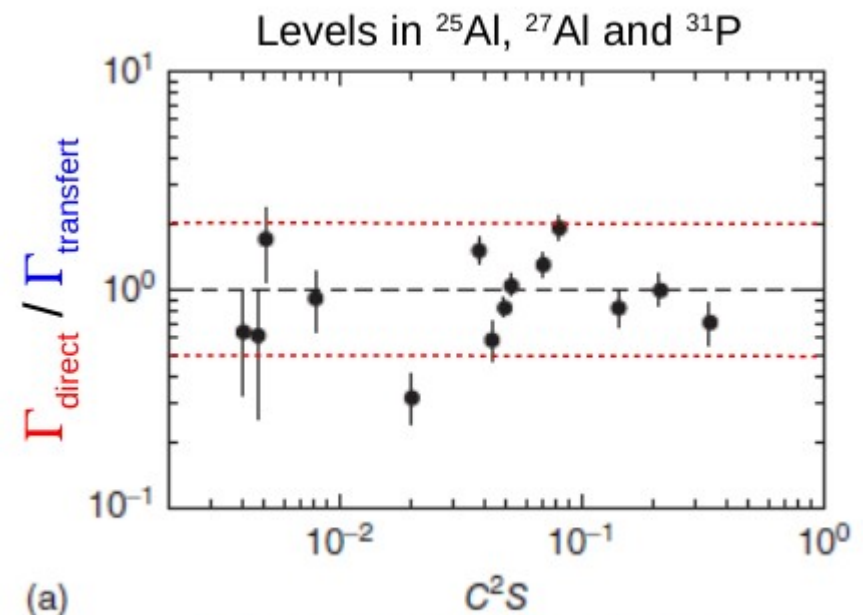
$$\Gamma_a = C^2 S_a \Gamma_a^{s.p.} = C^2 S_a \times \frac{\hbar^2 s}{\mu} |\mathcal{R}(s)|^2 P_l(E_r, s)$$

- Comparison of partial widths: transfer vs. direct:

**Direct:** (p,p) & (p,γ) reactions

**Transfer:** (3He,d) reaction

**Agreement within a factor 2**



Iliadis, Nuclear Physics of Stars (2015)

$\omega\gamma$ (eV)							$\omega\gamma$ (eV)		
7719.5	8	423.0	8	3	0.044	$2.48 \times 10^{-5}$	$7.42 \times 10^{-5}$	$(3/2, 5/2)^-$	$(1.14 \pm 0.25) \times 10^{-4}$ [11]
7737.3	7	440.8	7	3	0.114	$9.79 \times 10^{-5}$	$3.92 \times 10^{-4}$	$(5/2, 7/2)^-$	$\approx 3.72 \times 10^{-4}$ [35]
7781.1	8	484.6	8	1	0.015	0.061	0.123	$3/2^-$	$0.188 \pm 0.014$ [11]



# Resonance strengths

TABLE III. Properties of resonances above the  $^{30}\text{Si}+p$  threshold from the present work and comparison with the literature.

$E_x$ (keV)	$E_r^{c.m.}$ (keV)	Present work				Literature			Ref.
		$\ell$	$(2J+1)C^2S$	$\Gamma_p$ (eV)	$\omega\gamma$ (eV) <sup>a</sup>	$J^\pi$	$\ell$	$\omega\gamma$ (eV)	
7313.7 16	18.6 16			$1.45 \times 10^{-35}$ <sup>b</sup>	$1.45 \times 10^{-35}$	$(1/2, 3/2)^+$	0, 2	$\leq 6.50 \times 10^{-37}$	[35]
7316.2 9	19.6 9	3	0.0075	$2.94 \times 10^{-39}$	$1.18 \times 10^{-38}$	$(5/2, 7/2)^-$	3	$\approx 8.60 \times 10^{-40}$	[35]
7347.0 12	50.5 12	1	0.0007	$5.20 \times 10^{-21}$	$1.04 \times 10^{-20}$	$(3/2, 5/2)^-$	1, 3	$\leq 5.04 \times 10^{-17}$	[35]
7356 16	59.4 16								
7442.3 3	145.8 3			$4.33 \times 10^{-17}$ <sup>b</sup>	$2.60 \times 10^{-16}$	$11/2^+$	6	$\leq 1.24 \times 10^{-15}$	[35]
7445.7 27 <sup>c</sup>	149.2 29	2	0.0007	$1.16 \times 10^{-11}$	$2.33 \times 10^{-11}$	$(3/2^+, 5/2, 7/2, 9/2^+)$	2, 3, 4	$\leq 7.60 \times 10^{-8}$	[35]
7470.5 23	174.0 23	3	0.001	$1.59 \times 10^{-12}$	$6.38 \times 10^{-12}$	$(7/2, 9/2)^-$	3, 5	$\leq 1.27 \times 10^{-10}$	[35]
7572	275.5								
7691.1 10	394.6 10	3	0.006	$1.47 \times 10^{-6}$	$4.40 \times 10^{-6}$				[35]
7719.5 8	423.0 8	3	0.044	$2.48 \times 10^{-5}$	$7.42 \times 10^{-5}$	$(3/2, 5/2)^-$		$(1.14 \pm 0.25) \times 10^{-4}$	[11]
7737.3 7	440.8 7	3	0.114	$9.79 \times 10^{-5}$	$3.92 \times 10^{-4}$	$(5/2, 7/2)^-$	3	$\approx 3.72 \times 10^{-4}$	[35]
7781.1 8	484.6 8	1	0.015	0.061	0.123	$3/2^-$		$0.188 \pm 0.014$	[11]
7825 9	528.5 9								
7851.4 8	554.9 8	1	0.009	0.244	0.181 <sup>d</sup>				
7863.4 14	566.9 16	3	0.004	$5.55 \times 10^{-5}$	$1.67 \times 10^{-4}$				
7897.8 7	601.3 7	1	0.115	6.49		$1/2^-$		$1.95 \pm 0.10$	[42]

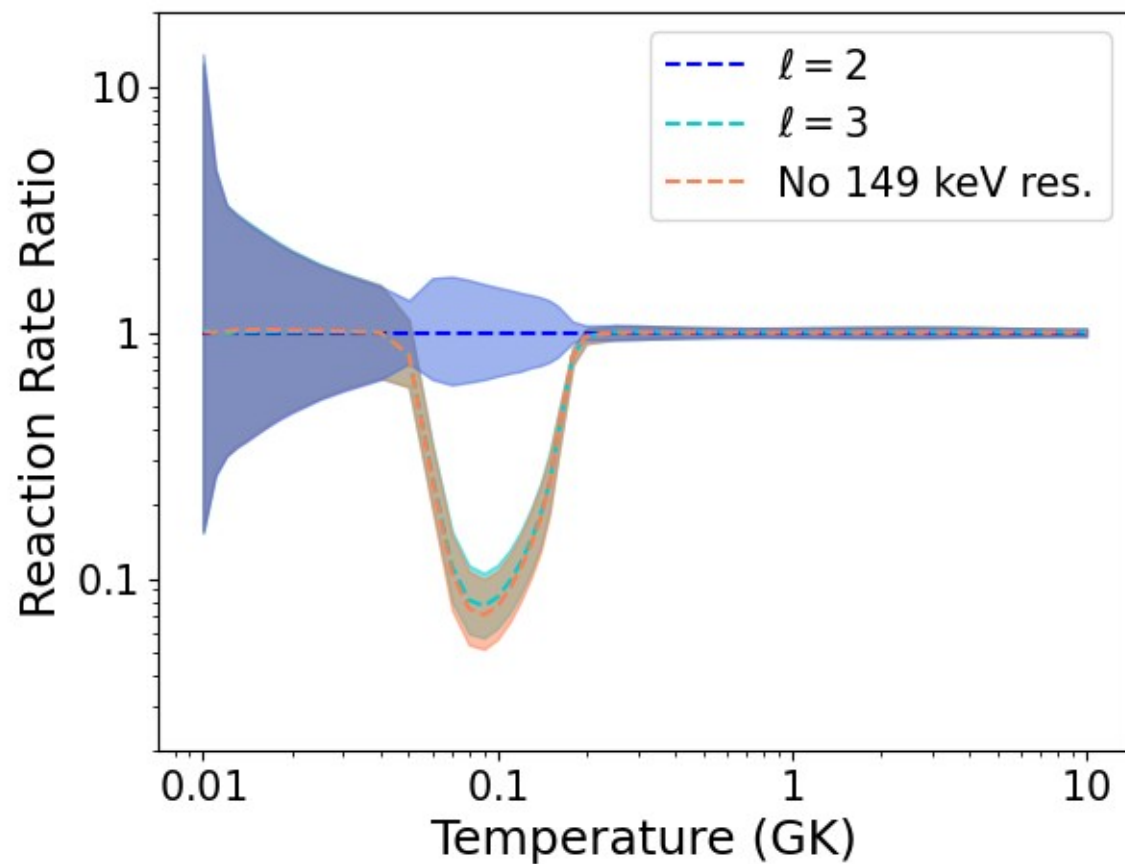
<sup>a</sup> Assuming  $\Gamma_p \ll \Gamma_\gamma$ , so that  $\omega\gamma = 0.5(2J+1)\Gamma_p$ .

<sup>b</sup> A dimensionless reduced width  $\langle\theta_p^2\rangle = 0.0045$  is assumed.

<sup>c</sup> 7441.4 keV in literature

<sup>d</sup> The complete resonance strength formula has been used (see text).

# 149 keV resonance



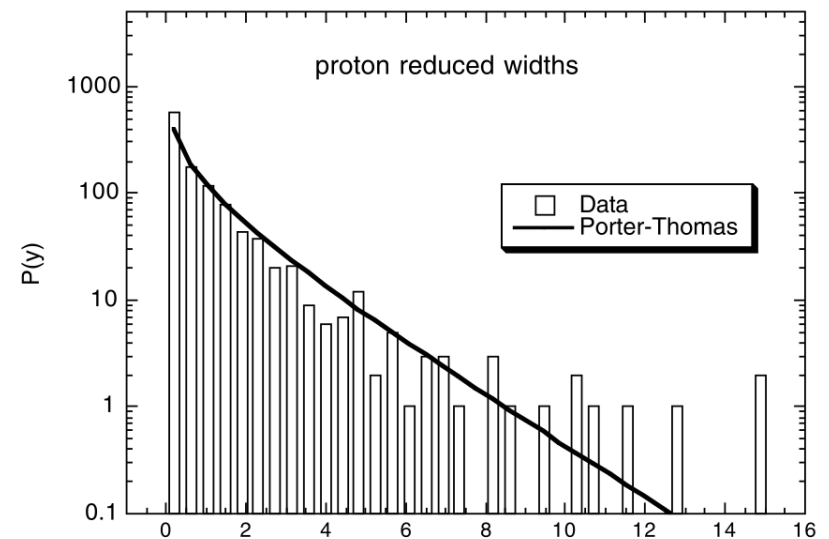
# RatesMC

Thermonuclear reaction rate for single and isolated narrow resonance :

$$\langle \sigma \nu \rangle \propto (\omega \gamma) e^{(-E_R/kT)}$$

$$\omega \gamma = \frac{2J_R + 1}{(2J_p + 1)(2J_{30Si} + 1)} \frac{\Gamma_p \Gamma_\gamma}{\Gamma}$$

- Resonance energies  $\rightarrow$  Normal distribution
- Resonance strengths or Partial widths  $\rightarrow$  Log-Normal distribution
- Not observed level: upper limits on widths  $\rightarrow$  Porter Thomas distribution



$$\Gamma_{sp} = 2P_{\ell}\gamma_{sp}^2, \quad \gamma_{sp}^2 = \frac{\hbar^2}{2\mu} |R(r)|^2$$

